

A NEW MIXED FINITE ELEMENT METHOD FOR THE CAHN-HILLIARD EQUATION *

ZHEN LIU [†], RUI MA [‡], AND MIN ZHANG [§]

Abstract. This paper presents a new mixed finite element method for the Cahn-Hilliard equation. The well-posedness of the mixed formulation is established and the error estimates for its linearized fully discrete scheme are provided. Numerical experiments are given to validate the efficiency and accuracy of the theoretical results.

Key words. Cahn-Hilliard, mixed finite element method, nonlinear problem, error estimates

MSC codes. 65M12, 65M60, 65Z05

1. Introduction. Let Ω be a bounded polyhedron in \mathbb{R}^3 or a polygon in \mathbb{R}^2 with the Lipschitz boundary $\partial\Omega$. This paper considers the Cahn-Hilliard equation

$$(1.1) \quad \left\{ \begin{array}{l} \frac{\partial u}{\partial t} - \Delta \left(-\Delta u + \frac{1}{\varepsilon^2} f(u) \right) = g(\mathbf{x}, t), \quad \text{in } \Omega \times (0, T], \\ \partial_n u = g_a(\mathbf{x}, t), \quad \text{on } \partial\Omega \times (0, T], \\ \partial_n \left(\Delta u - \frac{1}{\varepsilon^2} f(u) \right) = g_b(\mathbf{x}, t), \quad \text{on } \partial\Omega \times (0, T], \\ u(\mathbf{x}, 0) = u_0(\mathbf{x}), \quad \text{in } \Omega \times \{0\}. \end{array} \right.$$

Here the symbol Δ is the Laplacian operator, $T > 0$ is a fixed constant, and $\partial_n(\cdot)$ is the normal derivative where \mathbf{n} is the unit outward normal vector of $\partial\Omega$. The function $f(u)$ is the derivative of a smooth chemical potential $F(u)$, and the widely used Ginzburg-Landau double-well potential $F(u) = \frac{1}{4}(u^2 - 1)^2$ will be taken in this paper. The function $u_0(\mathbf{x})$ is the initial data. The functions $g(\mathbf{x}, t)$, $g_a(\mathbf{x}, t)$, $g_b(\mathbf{x}, t)$ serve as prescribed source terms assuming to be zero unless the contrary is explicitly stated.

The Cahn-Hilliard equation was introduced by Cahn and Hilliard [10] to describe the complicated phase separation and coarsening phenomena in a solid where only two different concentration phases can exist stably. The unknown function $u(\mathbf{x}, t)$ represents the concentration of each component and the parameter $\varepsilon > 0$ represents the inter-facial width. For more physical background and derivation of the Cahn-Hilliard equation, refer to [9, 47] and the references therein. The Cahn-Hilliard equation has been not only widely used in many complicated moving interface problems, multi-phase fluid flow and fluid dynamics [4, 56, 54], but also paired with other equations that describe physical behaviour of a given physical system, see, e.g., [1, 27, 36, 44].

Numerous studies on numerical methods have been conducted over the past thirty years, including finite element methods [22, 52], finite difference methods [50, 33, 37], finite volume methods [46, 6], and spectral methods [12, 15]. This paper focuses

*

Funding: The work of the second author was partially supported by NSFC project 12301466.

[†]LMAM and School of Mathematical Sciences, Peking University, Beijing 100871, P. R. China.
Chongqing Research Institute of Big Data, Peking University, Chongqing 401332, P. R. China.
(zliu37@pku.edu.cn).

[‡]Beijing Institute of Technology, Beijing 100081, P. R. China. (rui.ma@bit.edu.cn).

[§]College of Science, Beijing Forestry University, Beijing 100083, P. R. China. (zhang-mind01@bjfu.edu.cn).

on finite element methods for the Cahn-Hilliard equation. Ensuring C^1 continuity is imperative when directly discretizing this fourth-order equation with conforming elements. Elliott and French [22] employed the spline finite element space to establish a fully discrete scheme for 1D problem. However, it is much more difficult to preserve C^1 continuity in high-dimensional spaces. To alleviate spatial continuity requirements, an alternative strategy is to use nonstandard finite element methods, such as nonconforming element methods [23, 52, 57], discontinuous Galerkin methods [28, 29, 43], local discontinuous Galerkin methods [53], weak Galerkin methods [51] and virtual element methods [5]. Besides, based on the Ciarlet-Raviart mixed method [18] for biharmonic equations, the chemical potential was introduced as an auxiliary variable in [24] which splits the Cahn-Hilliard equation into two coupled problems involving second-order spatial derivatives. This gives rise to a mixed finite element method that employs only continuous finite elements. Various fully discrete schemes using this mixed finite element method for spatial discretization have been developed and analyzed, see, e.g., [21, 25, 19, 20, 16, 30].

However, the Ciarlet-Raviart method may yield spurious solutions for biharmonic equations on nonconvex domains, particularly with simply-supported boundary conditions [58]. This paper provides numerical examples which show that the Ciarlet-Raviart method yields spurious solutions with Cahn-Hilliard boundary conditions as well. Recently, a mixed finite element method that introduces the Hessian as an auxiliary variable has been developed, see, e.g., [48, 14, 40, 31]. Based on this method, this paper proposes a new mixed finite element method for the Cahn-Hilliard equation. The new mixed finite element method is suitable for various boundary conditions, including Cahn-Hilliard boundary conditions, even on nonconvex domain. Compared to nonconforming methods, the new mixed method offers a unified construction of finite elements in two, three, and even higher dimensions [13], while also allowing for arbitrary degrees of discretization.

The new mixed finite element method presented in this paper simultaneously seeks u and the introduced variable $\boldsymbol{\sigma} = \nabla^2 u - \frac{1}{\varepsilon^2} f(u)\mathbf{I}$, which is sought in $H(\text{divDiv}, \Omega; \mathbb{S})$, consisting of symmetric matrix-valued L^2 functions whose divDiv belongs to $L^2(\Omega)$, with proper boundary conditions. The well-posedness of the mixed formulation is established by demonstrating its equivalence to the primal formulation of the Cahn-Hilliard equation. Two distinct boundary conditions for the new mixed finite element method are explored. Specifically, one leads to an equivalent formula while the other is more sufficient. This paper mainly considers the latter boundary condition and employs the $H(\text{divDiv}, \Omega; \mathbb{S})$ conforming finite element in [40] for the discretization of $\boldsymbol{\sigma}$. Nevertheless, other $H(\text{divDiv}, \Omega; \mathbb{S})$ elements [14, 31] can also be employed. Besides, this paper provides detailed error estimates for the mixed finite element method. A key step in the proof is to utilize a broken H^2 -norm of the numerical solution u_h to control its L^∞ -norm. Mathematical induction is applied simultaneously to estimate the L^∞ -norm of u_h and the L^2 errors of $\boldsymbol{\sigma}_h$ and u_h . A postprocessing technique is employed to improve the convergence rates of $\boldsymbol{\sigma}_h$ and u_h . Numerical experiments are presented to validate the theoretical results.

This paper is organized as follows. Section 2 introduces some notations and lemmas. Section 3 presents the mixed formulation and provides its equivalence to the primal formulation. Section 4 gives the linearized fully discrete scheme of the mixed formulation and the error estimates. Section 5 provides numerical experiments to validate the theoretical results.

2. Preliminaries. Given a bounded domain $D \subset \mathbb{R}^d$ with $d = 2, 3$, let $L^p(D; X)$ denote the standard Lebesgue spaces of functions within D , taking values in space X , with the corresponding norm $\|\cdot\|_{L^p(D)}$. Similarly, let $H^m(D; X)$ denote the standard Sobolev spaces of functions for positive integers m with the corresponding norm $\|\cdot\|_{H^m(D)}$, and let $C^m(D; X)$ denote the space of m -times continuously differentiable functions. The L^2 -scalar product over D is denoted as $(\cdot, \cdot)_D$. The subscript D in $\|\cdot\|_{L^p(D)}$, $\|\cdot\|_{H^m(D)}$ and $(\cdot, \cdot)_D$ will be omitted if $D = \Omega$. In this paper, X could be \mathbb{R} , \mathbb{R}^d or \mathbb{S} , where \mathbb{S} denotes the set of symmetric $\mathbb{R}^{d \times d}$ matrices. If $X = \mathbb{R}$, then $L^2(D)$ abbreviates $L^2(D; X)$, similarly for $H^m(D)$ and $C^m(D)$. Let $H^{-m}(D)$ denote the dual space of $H_0^m(D)$ and $\langle \cdot, \cdot \rangle_{H^{-m} \times H_0^m}$ denote the duality product on $H^{-m}(D) \times H_0^m(D)$. Let Y be a real Banach space with the norm $\|\cdot\|_Y$. The space $L^\infty(0, T; Y)$ consists of all measurable functions $u : [0, T] \rightarrow Y$ with

$$(2.1) \quad \|u\|_{L^\infty(0, T; Y)} := \sup_{0 \leq t \leq T} \|u(t)\|_Y < \infty.$$

If $D \subset \mathbb{R}^3$ is a polyhedron, then let $\mathcal{F}(D), \mathcal{E}(D)$ and $\mathcal{V}(D)$ be the sets of all faces, edges and vertices of D , respectively. For a face $F \in \mathcal{F}(D)$, the unit outer normal vector \mathbf{n}_F is fixed. For any $F \in \mathcal{F}(D)$, let $\mathcal{E}(F)$ be the set of all edges of F . Specifically, for each $e \in \mathcal{E}(F)$, denote by $\mathbf{n}_{F,e}$ the unit vector parallel to F and outward normal to ∂F . Given an edge $e \in \mathcal{E}(D)$, the unit tangential vector \mathbf{t}_e , and two unit normal vectors, $\mathbf{n}_{e,1}$ and $\mathbf{n}_{e,2}$, are fixed. If $D \subset \mathbb{R}^2$ is a polygon, then let $\mathcal{E}(D)$ and $\mathcal{V}(D)$ be the sets of all edges and vertices of D , respectively. Given an edge $e \in \mathcal{E}(D)$, the unique unit outer normal vector \mathbf{n}_e and the unit tangential vector \mathbf{t}_e are fixed. In the absence of ambiguity, the symbol \mathbf{n} instead of \mathbf{n}_e and \mathbf{n}_F in two and three dimensions, respectively, will be used to denote the unit outer normal vector of ∂D . Let \mathbf{I} denote the identity matrix in \mathbb{R}^d . For $D \subset \mathbb{R}^3$, given $F \in \mathcal{F}(D)$, vector \mathbf{v} and tensor $\boldsymbol{\tau}$, define

$$(2.2) \quad \begin{aligned} \Pi_F \mathbf{v} &:= (\mathbf{I} - \mathbf{n}_F \mathbf{n}_F^T) \mathbf{v}, \\ \operatorname{div}_F(\boldsymbol{\tau} \mathbf{n}_F) &:= (\mathbf{n}_F \times \nabla) \cdot (\mathbf{n}_F \times (\boldsymbol{\tau} \mathbf{n}_F)). \end{aligned}$$

In this paper, the differential operator Div for matrix functions is applied row-wise. The following lemmas are presented for later use.

LEMMA 2.1 (Green's identity in 3D [14, 32]). *Suppose $\Omega \subset \mathbb{R}^3$. Let $\boldsymbol{\tau} \in H(\operatorname{div} \operatorname{Div}, \Omega; \mathbb{S}) \cap C^1(\bar{\Omega}; \mathbb{S})$ and $v \in H^2(\Omega)$. Then the following equality holds*

$$(2.3) \quad (\operatorname{div} \operatorname{Div} \boldsymbol{\tau}, v) = (\boldsymbol{\tau}, \nabla^2 v) - \sum_{F \in \mathcal{F}(\Omega)} (\boldsymbol{\tau} \mathbf{n}_F, \nabla v)_F + \sum_{F \in \mathcal{F}(\Omega)} (\mathbf{n}_F^T \operatorname{Div} \boldsymbol{\tau}, v)_F,$$

and furthermore

$$(2.4) \quad \begin{aligned} (\operatorname{div} \operatorname{Div} \boldsymbol{\tau}, v) &= (\boldsymbol{\tau}, \nabla^2 v) - \sum_{F \in \mathcal{F}(\Omega)} \sum_{e \in \mathcal{E}(F)} (\mathbf{n}_{F,e}^T \boldsymbol{\tau} \mathbf{n}_F, v)_e \\ &\quad - \sum_{F \in \mathcal{F}(\Omega)} \left[\left(\mathbf{n}_F^T \boldsymbol{\tau} \mathbf{n}_F, \frac{\partial v}{\partial \mathbf{n}_F} \right)_F - \left(2 \operatorname{div}_F(\boldsymbol{\tau} \mathbf{n}_F) + \frac{\partial (\mathbf{n}_F^T \boldsymbol{\tau} \mathbf{n}_F)}{\partial \mathbf{n}_F}, v \right)_F \right]. \end{aligned}$$

LEMMA 2.2 (Discrete Gronwall's inequality [38]). *Let τ, B and a_k, b_k, c_k, γ_k , for integers $k \geq 0$, be non-negative numbers such that*

$$a_n + \tau \sum_{k=0}^n b_k \leq \tau \sum_{k=0}^n \gamma_k a_k + \tau \sum_{k=0}^n c_k + B, \text{ for } n \geq 0,$$

suppose that $\tau\gamma_k < 1$, for all k , and set $\sigma_k = (1 - \tau\gamma_k)^{-1}$. Then

$$a_n + \tau \sum_{k=0}^n b_k \leq \exp\left(\tau \sum_{k=0}^n \gamma_k \sigma_k\right) \left(\tau \sum_{k=0}^n c_k + B\right), \text{ for } n \geq 0.$$

3. Mixed variational formulation. This section presents the new mixed variational formulation for the Cahn-Hilliard equation (1.1) and demonstrates its equivalence to the primal variational formulation.

Define

$$H_E^2(\Omega) := \{v \in H^2(\Omega) : \partial_n v = 0, \text{ on } \partial\Omega\}.$$

The primal formulation of (1.1) reads: Find $u \in H_E^2(\Omega)$ such that

$$(3.1) \quad \left(\frac{\partial u}{\partial t}, v\right) + (\nabla^2 u, \nabla^2 v) = \left(\frac{1}{\varepsilon^2} f(u) \mathbf{I}, \nabla^2 v\right), \quad \forall v \in H_E^2(\Omega).$$

According to [26, Theorem 2.1 and Remark 2], (3.1) possesses a unique solution for $f(u) = u^3 - u$ when $\partial\Omega$ is smooth enough.

Introducing the auxiliary variable

$$\boldsymbol{\sigma} := \nabla^2 u - \frac{1}{\varepsilon^2} f(u) \mathbf{I},$$

one can reformulate the Cahn-Hilliard equation (1.1) into

$$(3.2) \quad \begin{cases} \frac{\partial u}{\partial t} + \operatorname{div} \operatorname{Div} \boldsymbol{\sigma} = 0, & \text{in } \Omega \times (0, T], \\ \boldsymbol{\sigma} = \nabla^2 u - \frac{1}{\varepsilon^2} f(u) \mathbf{I}, & \text{in } \Omega \times (0, T], \\ \partial_n u = 0, & \text{on } \partial\Omega \times (0, T], \\ \operatorname{Div} \boldsymbol{\sigma} \cdot \mathbf{n} = 0, & \text{on } \partial\Omega \times (0, T], \\ u(\mathbf{x}, 0) = u_0(\mathbf{x}), & \text{on } \partial\Omega \times \{0\}. \end{cases}$$

Define

$$H(\operatorname{div} \operatorname{Div}, \Omega; \mathbb{S}) := \{\boldsymbol{\tau} \in L^2(\Omega; \mathbb{S}) : \operatorname{div} \operatorname{Div} \boldsymbol{\tau} \in L^2(\Omega)\},$$

equipped with the squared norm $\|\boldsymbol{\tau}\|_{H(\operatorname{div} \operatorname{Div})}^2 := \|\boldsymbol{\tau}\|_{L^2}^2 + \|\operatorname{div} \operatorname{Div} \boldsymbol{\tau}\|_{L^2}^2$. By employing a similar approach as presented in [32, 49], define a nonstandard Sobolev space with a portion of the trace vanishing as

$$(3.3) \quad \Sigma := \{\boldsymbol{\tau} \in H(\operatorname{div} \operatorname{Div}, \Omega; \mathbb{S}) : (\operatorname{div} \operatorname{Div} \boldsymbol{\tau}, v) = (\boldsymbol{\tau}, \nabla^2 v), \forall v \in H_E^2(\Omega)\}.$$

Let $V := L^2(\Omega)$. Then the new mixed variational formulation reads: Find $(\boldsymbol{\sigma}, u) \in \Sigma \times L^6(\Omega)$ such that

$$(3.4) \quad \begin{cases} \left(\frac{\partial u}{\partial t}, v\right) + (\operatorname{div} \operatorname{Div} \boldsymbol{\sigma}, v) = 0, & \forall v \in V, \\ (\boldsymbol{\sigma}, \boldsymbol{\tau}) - (\operatorname{div} \operatorname{Div} \boldsymbol{\tau}, u) = \left(-\frac{1}{\varepsilon^2} f(u) \mathbf{I}, \boldsymbol{\tau}\right), & \forall \boldsymbol{\tau} \in \Sigma. \end{cases}$$

Remark 3.1. The requirement $u \in L^6(\Omega)$ is reasonable since $f(u) = u^3 - u \in L^2(\Omega)$ requires at least $u \in L^6(\Omega)$. Indeed, the exact solution u of (3.1) belongs to $H^2(\Omega)$, implying $u \in L^6(\Omega)$.

The following two lemmas give the boundary conditions for smooth functions in Σ . Define the jump term for $F_1, F_2 \in \mathcal{F}(\Omega)$ and $F_1 \cap F_2 = e$ as

$$\llbracket \mathbf{n}_{F,e}^T \boldsymbol{\tau} \mathbf{n}_F \rrbracket_e := \mathbf{n}_{F_1,e}^T \boldsymbol{\tau} \mathbf{n}_{F_1} + \mathbf{n}_{F_2,e}^T \boldsymbol{\tau} \mathbf{n}_{F_2}.$$

LEMMA 3.2. *Suppose $\Omega \subset \mathbb{R}^3$. If $\boldsymbol{\tau} \in H(\operatorname{divDiv}, \Omega; \mathbb{S}) \cap C^1(\bar{\Omega}; \mathbb{S})$, then $\boldsymbol{\tau} \in \Sigma$ if and only if*

$$(3.5) \quad \begin{aligned} \llbracket \mathbf{n}_{F,e}^T \boldsymbol{\tau} \mathbf{n}_F \rrbracket_e &= 0, \quad \forall e \in \mathcal{E}(\Omega), \\ 2 \operatorname{div}_F(\boldsymbol{\tau} \mathbf{n}_F) + \frac{\partial (\mathbf{n}_F^T \boldsymbol{\tau} \mathbf{n}_F)}{\partial \mathbf{n}_F} &= 0, \quad \forall F \in \mathcal{F}(\Omega). \end{aligned}$$

Proof. For any $\boldsymbol{\tau} \in H(\operatorname{divDiv}, \Omega; \mathbb{S}) \cap C^1(\bar{\Omega}; \mathbb{S})$, Green's identity (2.4) shows

$$(3.6) \quad \begin{aligned} (\operatorname{divDiv} \boldsymbol{\tau}, v) &= (\boldsymbol{\tau}, \nabla^2 v) - \sum_{F \in \mathcal{F}(\Omega)} \sum_{e \in \mathcal{E}(F)} (\mathbf{n}_{F,e}^T \boldsymbol{\tau} \mathbf{n}_F, v)_e \\ &+ \sum_{F \in \mathcal{F}(\Omega)} \left(2 \operatorname{div}_F(\boldsymbol{\tau} \mathbf{n}_F) + \frac{\partial (\mathbf{n}_F^T \boldsymbol{\tau} \mathbf{n}_F)}{\partial \mathbf{n}_F}, v \right)_F, \end{aligned}$$

for all $v \in H_E^2(\Omega)$. If $\boldsymbol{\tau} \in \Sigma$, then the arbitrariness of v and (3.3) show that the boundary terms in (3.6) equal zero, which implies (3.5). On the contrary, if (3.5) holds, this and (3.6) lead to $\boldsymbol{\tau} \in \Sigma$. This concludes the proof. \square

Define the jump term for $e_1, e_2 \in \mathcal{E}(\Omega)$ and $e_1 \cap e_2 = \mathbf{x}$ as

$$\llbracket \mathbf{t}^T \boldsymbol{\tau} \mathbf{n} \rrbracket_{\mathbf{x}} := \operatorname{sign}_{e_1, \mathbf{x}} \mathbf{t}_{e_1}^T \boldsymbol{\tau} \mathbf{n}_{e_1} + \operatorname{sign}_{e_2, \mathbf{x}} \mathbf{t}_{e_2}^T \boldsymbol{\tau} \mathbf{n}_{e_2}$$

with

$$\operatorname{sign}_{e, \mathbf{x}} := \begin{cases} 1, & \text{if } \mathbf{x} \text{ is the end point of } e, \\ -1, & \text{if } \mathbf{x} \text{ is the start point of } e. \end{cases}$$

LEMMA 3.3. *Suppose $\Omega \subset \mathbb{R}^2$. If $\boldsymbol{\tau} \in H(\operatorname{divDiv}, \Omega; \mathbb{S}) \cap C^1(\bar{\Omega}; \mathbb{S})$, then $\boldsymbol{\tau} \in \Sigma$ if and only if*

$$(3.7) \quad \llbracket \mathbf{t}^T \boldsymbol{\tau} \mathbf{n} \rrbracket_{\mathbf{x}} = 0, \quad \forall \mathbf{x} \in \mathcal{V}(\Omega), \quad 2 \frac{\partial (\mathbf{t}_e^T \boldsymbol{\tau} \mathbf{n}_e)}{\partial \mathbf{t}_e} + \frac{\partial (\mathbf{n}_e^T \boldsymbol{\tau} \mathbf{n}_e)}{\partial \mathbf{n}_e} = 0, \quad \forall e \in \mathcal{E}(\Omega).$$

Proof. The proof is similar to that of Lemma 3.2 by using Green's identity in two dimensions [14, Lemma 4.2]. \square

The subsequent theorem shows the equivalence of the mixed formulation (3.4) and the primal one (3.1).

THEOREM 3.4. *The problems (3.1) and (3.4) are fully equivalent, i.e., if $u \in H_E^2(\Omega)$ solves (3.1), then $\boldsymbol{\sigma} = \nabla^2 u - \frac{1}{\varepsilon^2} f(u) \mathbf{I} \in \Sigma$ and $(\boldsymbol{\sigma}, u)$ solves (3.4). And, vice versa, if $(\boldsymbol{\sigma}, u) \in \Sigma \times V$ solves (3.4), then $u \in H_E^2(\Omega)$ and u solves (3.1).*

Proof. Suppose that $u \in H_E^2(\Omega)$ solves (3.1). Then $\boldsymbol{\sigma} = \nabla^2 u - \frac{1}{\varepsilon^2} f(u) \mathbf{I} \in L^2(\Omega; \mathbb{S})$ and

$$(3.8) \quad \left(\frac{\partial u}{\partial \mathbf{t}}, v \right) + (\boldsymbol{\sigma}, \nabla^2 v) = 0, \quad \forall v \in H_E^2(\Omega).$$

This and $C_0^\infty(\Omega) \subset H_E^2(\Omega)$ lead to $\operatorname{div}\operatorname{Div} \boldsymbol{\sigma} = -\frac{\partial u}{\partial t} \in L^2(\Omega)$. The first row in (3.4) immediately follows. This and (3.8) yield

$$(\boldsymbol{\sigma}, \nabla^2 v) = \left(-\frac{\partial u}{\partial t}, v\right) = (\operatorname{div}\operatorname{Div} \boldsymbol{\sigma}, v), \quad \forall v \in H_E^2(\Omega).$$

This shows $\boldsymbol{\sigma} \in \Sigma$. The definition of Σ and $u \in H_E^2(\Omega)$ imply

$$(\operatorname{div}\operatorname{Div} \boldsymbol{\tau}, u) = (\boldsymbol{\tau}, \nabla^2 u) = (\boldsymbol{\tau}, \boldsymbol{\sigma}) + \left(\frac{1}{\varepsilon^2} f(u) \mathbf{I}, \boldsymbol{\tau}\right), \quad \forall \boldsymbol{\tau} \in \Sigma,$$

which proves the second row in (3.4).

Suppose that $(\boldsymbol{\sigma}, u) \in \Sigma \times L^6(\Omega)$ solves (3.4). Since $\boldsymbol{\sigma} + \frac{1}{\varepsilon^2} f(u) \mathbf{I} \in L^2(\Omega; \mathbb{S})$ and $C_0^\infty(\Omega; \mathbb{S}) \subset \Sigma$, it follows from the second row of (3.4) that $\nabla^2 u = \boldsymbol{\sigma} + \frac{1}{\varepsilon^2} f(u) \mathbf{I} \in L^2(\Omega; \mathbb{S})$. This and Lemma 4.4 imply $u \in H^2(\Omega)$. The choice of $v \in H_E^2(\Omega)$ in the first row of (3.4) derives that u solves (3.1) since

$$\begin{aligned} \left(\frac{\partial u}{\partial t}, v\right) &= -(\operatorname{div}\operatorname{Div} \boldsymbol{\sigma}, v) = -(\boldsymbol{\sigma}, \nabla^2 v) \\ &= -(\nabla^2 u, \nabla^2 v) + \left(\frac{1}{\varepsilon^2} f(u) \mathbf{I}, v\right), \quad \forall v \in H_E^2(\Omega). \end{aligned}$$

It remains to show $u \in H_E^2(\Omega)$. The second row in (3.4) implies

$$(\nabla^2 u, \boldsymbol{\tau}) = (\operatorname{div}\operatorname{Div} \boldsymbol{\tau}, u)$$

for any $\boldsymbol{\tau} \in C^1(\bar{\Omega}; \mathbb{S}) \cap \Sigma$. This, Green's identity in Lemma 2.1, and Lemma 3.2 show $\partial_n u = 0$ for $\Omega \subset \mathbb{R}^3$. Similarly, Green's identity in [14, Lemma 4.2] and Lemma 3.3 show $\partial_n u = 0$ for $\Omega \subset \mathbb{R}^2$. This concludes the proof. \square

Recall Π_F from (2.2). This paper will use the following more sufficient boundary conditions compared with those in (3.5) and (3.7) for the mixed finite element method.

LEMMA 3.5. *Suppose $\Omega \subset \mathbb{R}^3$. If $\boldsymbol{\tau} \in H(\operatorname{div}\operatorname{Div}, \Omega; \mathbb{S}) \cap C^1(\bar{\Omega}; \mathbb{S})$ satisfies*

$$(3.9) \quad \Pi_F(\boldsymbol{\tau} \mathbf{n}_F) = 0, \quad \mathbf{n}_F^\top \operatorname{Div} \boldsymbol{\tau} = 0, \quad \forall F \in \mathcal{F}(\Omega),$$

then $\boldsymbol{\tau} \in \Sigma$. Similarly, for $\Omega \subset \mathbb{R}^2$, if $\boldsymbol{\tau} \in H(\operatorname{div}\operatorname{Div}, \Omega; \mathbb{S}) \cap C^1(\bar{\Omega}; \mathbb{S})$ satisfies $\mathbf{t}_e^\top \boldsymbol{\tau} \mathbf{n}_e = 0$ and $\mathbf{n}_e^\top \operatorname{Div} \boldsymbol{\tau} = 0$ for all $e \in \mathcal{E}(\Omega)$, then $\boldsymbol{\tau} \in \Sigma$.

Proof. Substituting (3.9) into Green's identity (2.3) proves $\boldsymbol{\tau} \in \Sigma$ for $\Omega \subset \mathbb{R}^3$. Similar arguments suit for $\Omega \subset \mathbb{R}^2$. \square

Remark 3.6. The conditions in Lemma 3.5 are reasonable due to the exact solution $(\boldsymbol{\sigma}, u)$ satisfies those conditions as well.

4. Mixed finite element method. This section establishes the linearized fully discrete scheme of (3.4) and presents the error estimates.

4.1. Linearized fully discrete scheme. Let N be a positive integer and let $\{t^n\}_{n=0}^N$ constitute a uniform partition of $[0, T]$ with the step size $\tau = \frac{T}{N}$. Select the backward Euler method as the temporal discretization method and incorporate the nonlinear term in the last time step. Then, the first-order semi-implicit method reads: Find $(\hat{\boldsymbol{\sigma}}^n, \hat{u}^n) \in \Sigma \times L^6(\Omega)$ such that for $n = 1, 2, \dots, N$,

$$\begin{cases} \frac{1}{\tau}(\hat{u}^n - \hat{u}^{n-1}, v) + (\operatorname{div}\operatorname{Div} \hat{\boldsymbol{\sigma}}^n, v) = 0, & \forall v \in V, \\ (\hat{\boldsymbol{\sigma}}^n, \boldsymbol{\tau}) - (\operatorname{div}\operatorname{Div} \boldsymbol{\tau}, \hat{u}^n) = \left(-\frac{1}{\varepsilon^2} f(\hat{u}^{n-1}) \mathbf{I}, \boldsymbol{\tau}\right), & \forall \boldsymbol{\tau} \in \Sigma. \end{cases}$$

At the initial time step, let $\hat{u}^0(\mathbf{x}, 0) = u_0(\mathbf{x})$.

Suppose that \mathcal{T}_h is a shape regular and quasi-uniform subdivision of Ω consisting of triangles in two dimensions and tetrahedrons in three dimensions. Define h as the maximum of the diameters of all the elements $K \in \mathcal{T}_h$. The jump of u across an interior $d-1$ face G shared by neighboring elements K_+ and K_- is defined by $[u]_G := (u|_{K_+} - u|_{K_-})|_G$. When it comes to any boundary face $G \subset \partial\Omega$, the jump $[\cdot]_G$ reduces to the trace. For $\Omega \subset \mathbb{R}^3$, let $\mathcal{V}_h, \mathcal{E}_h, \mathcal{F}_h, \mathcal{V}_h^i, \mathcal{E}_h^i, \mathcal{F}_h^i$ denote the set of all the vertices, the edges, the faces, the interior vertices, the interior edges, the interior faces of \mathcal{T}_h , respectively. Let h_e, h_F and h_K denote the diameters of $e \in \mathcal{E}_h, F \in \mathcal{F}_h$ and $K \in \mathcal{T}_h$, respectively. For $\Omega \subset \mathbb{R}^2$, the sets \mathcal{F}_h and \mathcal{F}_h^i are empty and h_F has no meaning.

To give the discrete spaces, introduce the $H(\text{div}, \Omega; \mathbb{S})$ conforming spaces in [41, 42, 39] with $k \geq 3$ as follows

$$\mathcal{U}_{\partial K, b} := \{ \boldsymbol{\tau} \in P_k(K; \mathbb{S}) : \boldsymbol{\tau} \mathbf{n} = 0, \text{ on } \partial K \},$$

$$\begin{aligned} \mathcal{U}_{k, h} := \{ \boldsymbol{\tau} \in H(\text{div}, \Omega; \mathbb{S}) : \boldsymbol{\tau} = \boldsymbol{\tau}_c + \boldsymbol{\tau}_b, \boldsymbol{\tau}_c \in H^1(\Omega; \mathbb{S}), \\ \boldsymbol{\tau}_c|_K \in P_k(K; \mathbb{S}), \boldsymbol{\tau}_b|_K \in \mathcal{U}_{\partial K, b}, \forall K \in \mathcal{T}_h \}. \end{aligned}$$

Introduce the $H(\text{div}, \Omega; \mathbb{S}) \cap H(\text{divDiv}, \Omega; \mathbb{S})$ conforming spaces in [40] with zero boundary conditions in \mathbb{R}^3 as

$$\Sigma_h := \{ \boldsymbol{\tau}_h \in \mathcal{U}_{k, h} : \Pi_F(\boldsymbol{\tau}_h \mathbf{n}_F) = 0, \forall F \in \mathcal{F}_h \setminus \mathcal{F}_h^i, [\text{Div } \boldsymbol{\tau}_h \cdot \mathbf{n}_F]_F = 0, \forall F \in \mathcal{F}_h \},$$

and in \mathbb{R}^2 as

$$\Sigma_h := \{ \boldsymbol{\tau}_h \in \mathcal{U}_{k, h} : \mathbf{t}_e^T \boldsymbol{\tau}_h \mathbf{n}_e|_e = 0, \forall e \in \mathcal{E}_h \setminus \mathcal{E}_h^i, [\text{Div } \boldsymbol{\tau}_h \cdot \mathbf{n}_e]_e = 0, \forall e \in \mathcal{E}_h \}.$$

Define the piecewise polynomial spaces

$$V_h := \{ v_h \in L^2(\Omega) : v_h|_K \in P_{k-2}(K), \forall K \in \mathcal{T}_h \},$$

equipped with the mesh-dependent semi-norm in \mathbb{R}^3 as

$$|v_h|_{2, h}^2 := \sum_{K \in \mathcal{T}_h} |v_h|_{H^2(K)}^2 + \sum_{F \in \mathcal{F}_h^i} h_F^{-3} \|[v_h]_F\|_{L^2(F)}^2 + \sum_{F \in \mathcal{F}_h} h_F^{-1} \|[\partial_n v_h]_F\|_{L^2(F)}^2,$$

and in \mathbb{R}^2 as

$$|v_h|_{2, h}^2 := \sum_{K \in \mathcal{T}_h} |v_h|_{H^2(K)}^2 + \sum_{e \in \mathcal{E}_h^i} h_e^{-3} \|[v_h]_e\|_{L^2(e)}^2 + \sum_{e \in \mathcal{E}_h} h_e^{-1} \|[\partial_n v_h]_e\|_{L^2(e)}^2.$$

The following lemma holds for the mesh-dependent semi-norm which will be used in the error estimates.

LEMMA 4.1. *There exists some constant $\beta > 0$ such that the following inf-sup condition holds*

$$(4.1) \quad \sup_{\boldsymbol{\tau}_h \in \Sigma_h} \frac{(\text{divDiv } \boldsymbol{\tau}_h, v_h)}{\|\boldsymbol{\tau}_h\|_{L^2}} \geq \beta |v_h|_{2, h}, \quad \forall v_h \in V_h.$$

Proof. Based on [40, Lemma 3.4], one can construct a $\boldsymbol{\tau}_h \in \Sigma_h$ on each $K \in \mathcal{T}_h$ in \mathbb{R}^3 with modifications

$$\begin{aligned} (\mathbf{n}_F^T \boldsymbol{\tau}_h \mathbf{n}_F, q)_F &= (h_F^{-1} [\partial_n v_h]_F, q)_F, & \forall q \in P_{k-3}(F), F \in \mathcal{F}(K), \\ (\mathbf{t}_{F,i}^T \boldsymbol{\tau}_h \mathbf{n}_F, q)_F &= 0, & \forall q \in P_{k-3}(F), F \in \mathcal{F}(K), \\ (\text{Div } \boldsymbol{\tau}_h \cdot \mathbf{n}_F, q)_F &= -(h_F^{-3} [v_h]_F, q)_F, & \forall q \in P_{k-1}(F), F \in \mathcal{F}(K) \cap \mathcal{F}_h^i, \\ (\text{Div } \boldsymbol{\tau}_h \cdot \mathbf{n}_F, q)_F &= 0, & \forall q \in P_{k-1}(F), F \in \mathcal{F}(K) \cap (\mathcal{F}_h \setminus \mathcal{F}_h^i). \end{aligned}$$

These modifications lead to

$$(4.2) \quad (\text{divDiv } \boldsymbol{\tau}_h, v_h) = |v_h|_{2,h}^2.$$

The scaling argument leads to $\|\boldsymbol{\tau}_h\|_{L^2} \leq C|v_h|_{2,h}$ with a positive constant C . This and (4.2) prove (4.1) in \mathbb{R}^3 with $\beta = \frac{1}{C}$. Similar arguments prove (4.1) in \mathbb{R}^2 . \square

Then, given the solution at time t^{n-1} , the fully discrete scheme seeks $(\boldsymbol{\sigma}_h^n, u_h^n) \in (\Sigma_h, V_h)$ such that for $n = 1, 2, \dots, N$,

$$(4.3) \quad \begin{cases} \frac{1}{\tau}(u_h^n - u_h^{n-1}, v_h) + (\text{divDiv } \boldsymbol{\sigma}_h^n, v_h) = 0, & \forall v_h \in V_h, \\ (\boldsymbol{\sigma}_h^n, \boldsymbol{\tau}_h) - (\text{divDiv } \boldsymbol{\tau}_h, u_h^n) = \left(-\frac{1}{\varepsilon^2} f(u_h^{n-1}) \mathbf{I}, \boldsymbol{\tau}_h\right), & \forall \boldsymbol{\tau}_h \in \Sigma_h. \end{cases}$$

At the initial time step, let

$$u_h^0 = \Pi_h u_0, \quad \boldsymbol{\sigma}_h^0 = \Pi_h \boldsymbol{\sigma}_0 = \Pi_h \left(\nabla^2 u_0 - \frac{1}{\varepsilon^2} f(u_0) \mathbf{I} \right),$$

where the projection operator Π_h will be defined in (4.4) below.

Remark 4.2. Note that the exact solution u satisfies mass conservation

$$\frac{\partial}{\partial t} \int_{\Omega} u dx = \int_{\Omega} \Delta \left(-\Delta u + \frac{1}{\varepsilon^2} f(u) \right) dx = \int_{\partial\Omega} \partial_n \left(-\Delta u + \frac{1}{\varepsilon^2} f(u) \right) dx = 0.$$

By taking $v_h = 1$ in (4.3), it can be observed from the first row that $\int_{\Omega} u_h^n dx = \int_{\Omega} u_h^{n-1} dx$.

Define the space

$$V_h^0 := \left\{ v_h \in V_h : \int_{\Omega} v_h dx = 0 \right\}.$$

Note that the semi-norm $|\cdot|_{2,h}$ of V_h is a norm of V_h^0 . To give the error estimates, introduce the projection operator $\Pi_h : (\Sigma, V) \rightarrow (\Sigma_h, V_h)$, for given exact solution $(\boldsymbol{\sigma}, u)$ of (3.4) at any time, such that $(\Pi_h \boldsymbol{\sigma}, \Pi_h u) \in (\Sigma_h, V_h)$ with $\int_{\Omega} \Pi_h u dx = \int_{\Omega} u dx$ satisfies

$$(4.4) \quad \begin{cases} (\text{divDiv } (\Pi_h \boldsymbol{\sigma} - \boldsymbol{\sigma}), v_h) = 0, & \forall v_h \in V_h^0, \\ (\Pi_h \boldsymbol{\sigma} - \boldsymbol{\sigma}, \boldsymbol{\tau}_h) - (\text{divDiv } \boldsymbol{\tau}_h, \Pi_h u - u) = 0, & \forall \boldsymbol{\tau}_h \in \Sigma_h. \end{cases}$$

Denote the projection error functions as

$$\boldsymbol{\theta}_{\boldsymbol{\sigma}} := \boldsymbol{\sigma} - \Pi_h \boldsymbol{\sigma}, \quad \boldsymbol{\theta}_u := u - \Pi_h u.$$

The estimates of $\boldsymbol{\theta}_{\boldsymbol{\sigma}}$ and $\boldsymbol{\theta}_u$ will be given in the subsequent subsection by proving the discrete inf-sup condition of (4.4).

4.2. Estimates of θ_σ and θ_u . Compared to the well-posedness in [40, Theorem 3.1], this paper needs to deal with extra boundary conditions. Recall that $\mathcal{F}(\Omega)$ and $\mathcal{E}(\Omega)$ denote the sets of all faces and edges of Ω , respectively. Define the space Σ_0 in \mathbb{R}^3 as

$$\Sigma_0 := \{\boldsymbol{\tau} \in H^1(\Omega; \mathbb{S}) : \Pi_F(\boldsymbol{\tau} \mathbf{n}_F) = 0, \forall F \in \mathcal{F}(\Omega)\},$$

and in \mathbb{R}^2 as

$$\Sigma_0 := \{\boldsymbol{\tau} \in H^1(\Omega; \mathbb{S}) : \mathbf{t}_e^\top \boldsymbol{\tau} \mathbf{n}_e|_e = 0, \forall e \in \mathcal{E}(\Omega)\}.$$

For $\mathbf{v} \in L^2(\Omega; \mathbb{R}^d)$, define its symmetric gradient as $\nabla_s \mathbf{v} := \frac{1}{2}(\nabla \mathbf{v} + \nabla \mathbf{v}^\top)$. The following lemma is crucial to the proof of the discrete inf-sup condition of (4.4).

LEMMA 4.3. *For any $v_h \in V_h^0$, there exists a matrix-valued function $\boldsymbol{\tau} \in \Sigma_0$ such that $\text{div Div } \boldsymbol{\tau} = v_h$ and*

$$(4.5) \quad \text{Div } \boldsymbol{\tau} \in H_0^1(\Omega; \mathbb{R}^d), \quad \|\boldsymbol{\tau}\|_{H^1} + \|\text{Div } \boldsymbol{\tau}\|_{H^1} \leq C \|v_h\|_{L^2},$$

for some generic constant C .

The proof of Lemma 4.3 requires the following two lemmas.

LEMMA 4.4 (Korn's inequality [3, Theorem 3.2]). *There exists a constant $C > 0$ such that*

$$\|\mathbf{v}\|_{L^2} \leq C (\|\mathbf{v}\|_{H^{-1}} + \|\nabla_s \mathbf{v}\|_{H^{-1}}), \quad \forall \mathbf{v} \in L^2(\Omega; \mathbb{R}^3).$$

LEMMA 4.5 ([17, Theorem 6.3-4]). *If $\mathbf{v} \in L^2(\Omega; \mathbb{R}^3)$ satisfies $\|\nabla_s \mathbf{v}\|_{H^{-1}} = 0$, then \mathbf{v} is a rigid motion function in \mathbb{R}^3 , i.e., there exist two vectors $\mathbf{a}, \mathbf{b} \in \mathbb{R}^3$ such that $\mathbf{v}(\mathbf{x}) = \mathbf{a} + \mathbf{b} \times \mathbf{x}$.*

Analogous arguments will show that Lemma 4.4-4.5 hold for $\Omega \subset \mathbb{R}^2$ as well. If $\mathbf{v} \in L^2(\Omega; \mathbb{R}^2)$ satisfies $\|\nabla_s \mathbf{v}\|_{H^{-1}} = 0$, then there exist constants $a, b, c \in \mathbb{R}$ such that $\mathbf{v}(\mathbf{x}) = \begin{pmatrix} a - cy \\ b + cx \end{pmatrix}$.

Proof of Lemma 4.3. The proof for $\Omega \subset \mathbb{R}^2$ is similar to that for $\Omega \subset \mathbb{R}^3$ which is detailed here. For any $v_h \in V_h^0$, there exists a $\boldsymbol{\psi} \in H_0^1(\Omega; \mathbb{R}^d)$ such that $\text{div } \boldsymbol{\psi} = v_h$ [35]. It remains to prove the inf-sup condition

$$(4.6) \quad \sup_{\boldsymbol{\tau} \in \Sigma_0} \frac{(\text{Div } \boldsymbol{\tau}, \boldsymbol{\phi})}{\|\boldsymbol{\tau}\|_{H^1}} \geq \beta \|\boldsymbol{\phi}\|_{L^2}, \quad \forall \boldsymbol{\phi} \in L^2(\Omega; \mathbb{R}^d).$$

Assume that (4.6) is not valid. Then there would exist a sequence $\{\boldsymbol{\phi}_n\}$ in L^2 such that $\|\boldsymbol{\phi}_n\|_{L^2} = 1$ and

$$(4.7) \quad \lim_{n \rightarrow \infty} \sup_{\boldsymbol{\tau} \in \Sigma_0} \frac{(\text{Div } \boldsymbol{\tau}, \boldsymbol{\phi}_n)}{\|\boldsymbol{\tau}\|_{H^1}} = 0.$$

The first thing is to prove $\{\boldsymbol{\phi}_n\}$ is a Cauchy sequence in L^2 . Lemma 4.4 shows

$$(4.8) \quad \|\boldsymbol{\phi}_n - \boldsymbol{\phi}_m\|_{L^2} \leq \|\boldsymbol{\phi}_n - \boldsymbol{\phi}_m\|_{H^{-1}} + \|\nabla_s(\boldsymbol{\phi}_n - \boldsymbol{\phi}_m)\|_{H^{-1}}.$$

The Rellich-Kondrachev compact embedding theorem [2] $H^1 \xhookrightarrow{c} L^2 \xhookrightarrow{c} H^{-1}$ and $\|\boldsymbol{\phi}_n\|_{L^2} = 1$ imply that $\{\boldsymbol{\phi}_n\}$ is a Cauchy sequence in H^{-1} . Additionally,

$$(4.9) \quad \begin{aligned} \|\nabla_s(\boldsymbol{\phi}_n - \boldsymbol{\phi}_m)\|_{H^{-1}} &= \sup_{\boldsymbol{\tau} \in H_0^1(\Omega; \mathbb{S})} \frac{(\nabla_s(\boldsymbol{\phi}_n - \boldsymbol{\phi}_m), \boldsymbol{\tau})_{H^{-1} \times H^1}}{\|\boldsymbol{\tau}\|_{H^1}} \\ &= \sup_{\boldsymbol{\tau} \in H_0^1(\Omega; \mathbb{S})} \frac{(\text{Div } \boldsymbol{\tau}, \boldsymbol{\phi}_n - \boldsymbol{\phi}_m)}{\|\boldsymbol{\tau}\|_{H^1}}. \end{aligned}$$

This, $H_0^1(\Omega; \mathbb{S}) \subset \Sigma_0$, and (4.7) imply that $\{\nabla_s \phi_n\}$ is a Cauchy sequence in H^{-1} . The previous arguments and (4.8) show that there exists a $\phi \in L^2(\Omega; \mathbb{R}^d)$ such that $\lim_{n \rightarrow \infty} \phi_n = \phi$ in L^2 and $\|\phi\|_{L^2} = 1$. A triangle inequality leads to

$$(4.10) \quad \|\nabla_s \phi\|_{H^{-1}} \leq \|\nabla_s(\phi - \phi_n)\|_{H^{-1}} + \|\nabla_s \phi_n\|_{H^{-1}}.$$

Proceeding as in (4.9) shows

$$(4.11) \quad \lim_{n \rightarrow \infty} \|\nabla_s \phi_n\|_{H^{-1}} = 0.$$

Since $\|\nabla_s(\phi - \phi_n)\|_{H^{-1}} \leq \|\phi - \phi_n\|_{L^2}$, (4.10)-(4.11) lead to $\|\nabla_s \phi\|_{H^{-1}} = 0$. The combination with Lemma 4.5 implies that ϕ is a rigid motion function. Since $\|\phi\|_{L^2} = 1$ and $\mathbf{n}^T \phi \neq 0$ on $\partial\Omega$, there exists a $\tau_1 \in \Sigma_0$ such that $(\text{Div } \tau_1, \phi) = -(\tau_1 \mathbf{n}, \phi)_{\partial\Omega} = -(\mathbf{n}^T \tau_1 \mathbf{n}, \mathbf{n}^T \phi)_{\partial\Omega} > 0$, which contradicts (4.7). This proves (4.6), and implies the existence of a desired τ with $\text{Div } \tau = \psi$. This concludes the proof. \square

Lemma 4.3 gives rise to the following discrete inf-sup condition of (4.4).

THEOREM 4.6. *There exists a constant $\beta > 0$ such that*

$$\sup_{\tau_h \in \Sigma_h} \frac{(\text{div Div } \tau_h, v_h)}{\|\tau_h\|_{H(\text{div Div})}} \geq \beta \|v_h\|_{L^2}, \quad \forall v_h \in V_h^0.$$

Proof. Given any $v_h \in V_h^0$, Lemma 4.3 shows that there exists a $\tau \in \Sigma_0$ such that $\text{div Div } \tau = v_h$ and τ satisfies (4.5). Define an interpolation operator $\tilde{\Pi}_h$ in \mathbb{R}^3 as in [40, Subsec. 3.1] with modifications

$$\tilde{\Pi}_h \tau(a) = 0, \quad \forall a \in \mathcal{V}_h \setminus \mathcal{V}_h^i,$$

$$\mathbf{t}_e^T (\tilde{\Pi}_h \tau) \mathbf{n}_{e,j} = 0, \mathbf{n}_{e,i}^T (\tilde{\Pi}_h \tau) \mathbf{n}_{e,j} = 0, \quad \forall e \in \mathcal{E}_h \setminus \mathcal{E}_h^i, 1 \leq i, j \leq 2,$$

and in \mathbb{R}^2 with modifications

$$\tilde{\Pi}_h \tau(a) = 0, \quad \forall a \in \mathcal{V}_h \setminus \mathcal{V}_h^i.$$

Then the modified interpolation operator $\tilde{\Pi}_h$ preserves the zero boundary conditions in Lemma 3.5 so that $\tilde{\Pi}_h \tau \in \Sigma_h$ and $\text{div Div } \tilde{\Pi}_h \tau = \text{div Div } \tau = v_h$. The boundedness

$$\|\tilde{\Pi}_h \tau\|_{L^2} \leq C(\|\tau\|_{H^1} + \|\text{Div } \tau\|_{H^1}),$$

and (4.5) conclude the proof. \square

The estimates for the projection error functions θ_σ and θ_u can be obtained immediately from Lemma 4.1 and Theorem 4.6.

LEMMA 4.7. *For $k \geq 3$, it holds*

$$(4.12a) \quad \|\theta_u\|_{L^2} + \|\theta_\sigma\|_{L^2} \leq Ch^{k-1} \|u\|_{H^{k+1}},$$

$$(4.12b) \quad \left\| \frac{\partial \theta_u}{\partial t} \right\|_{L^2} + \left\| \frac{\partial \theta_\sigma}{\partial t} \right\|_{L^2} \leq Ch^{k-1} \left\| \frac{\partial u}{\partial t} \right\|_{H^{k+1}},$$

$$(4.12c) \quad |\theta_u|_{2,h} \leq Ch^{k-3} \|u\|_{H^{k+1}}.$$

Proof. Theorem 4.6 and Babuška Brezzi theory [7] lead to the well-posedness of (4.4), which proves (4.12a). The derivation of (4.4) with respect to t yields analogous equations of $\frac{\partial \theta_\sigma}{\partial t}$ and $\frac{\partial \theta_u}{\partial t}$. Similar arguments prove (4.12b). Lemma 4.1 and Babuška Brezzi theory lead to (4.12c). \square

4.3. Error Estimates. This subsection derives the error estimates for the linearized fully discrete mixed scheme (4.3). For the convenience of the error analysis, assume that the solution $u(\mathbf{x}, t)$ of (3.2) satisfies the following regularities

$$(4.13) \quad u \in L^\infty(0, T; H^{k+1}), \quad \frac{\partial u}{\partial t} \in L^\infty(0, T; H^{k+1}), \quad \frac{\partial^2 u}{\partial t^2} \in L^\infty(0, T; L^2).$$

According to (2.1), there exists a uniform bound M independent of n, h, τ such that

$$(4.14) \quad \sup_{0 \leq t \leq T} \left\{ \|u\|_{L^\infty}, \|u\|_{H^{k+1}}, \left\| \frac{\partial u}{\partial t} \right\|_{H^{k+1}}, \left\| \frac{\partial^2 u}{\partial t^2} \right\|_{L^2} \right\} \leq M.$$

Let $(\boldsymbol{\sigma}^n, u^n)$ denote the value of the exact solution $(\boldsymbol{\sigma}, u)$ at the time step n . Let $\theta_{\boldsymbol{\sigma}}^n, \theta_u^n$ denote the value of $\theta_{\boldsymbol{\sigma}}, \theta_u$ at the time step n . With the estimates of $\theta_{\boldsymbol{\sigma}}^n$ and θ_u^n in Lemma 4.7, it remains to estimate

$$e_{\boldsymbol{\sigma}}^n := \Pi_h \boldsymbol{\sigma}^n - \boldsymbol{\sigma}_h^n, \quad e_u^n := \Pi_h u^n - u_h^n, \quad \text{for } n = 0, 1, 2, \dots, N.$$

The following lemma will be used in the estimates.

LEMMA 4.8. *There exists a constant C independent of h and τ such that*

$$(4.15) \quad \|v_h\|_{L^\infty} \leq C |v_h|_{2,h}, \quad \forall v_h \in V_h.$$

Proof. This follows with the arguments of [8, Lemma 3.7] on the enriching operators $E : V_h \rightarrow H^2(\Omega)$ [11, 34, 59]. Further details are omitted for brevity. \square

To establish the error estimates for the fully discrete scheme (4.3), a key result is needed: $\|e_u^n\|_{L^\infty}$ is bounded. The proof of the following theorem uses mathematical induction to assert this result and then establishes the error estimates based on this result.

THEOREM 4.9. *Under the regularity assumption (4.13), there exist two positive constants h_0 and τ_0 such that when $h < h_0$ and $\tau < \tau_0$, (4.3) is uniquely solvable with $k \geq 3$ and the following error estimate holds*

$$(4.16) \quad \max_{0 \leq n \leq N} \left(\|e_u^n\|_{L^2}^2 + \sum_{i=1}^n \tau \|e_{\boldsymbol{\sigma}}^i\|_{L^2}^2 \right) \leq C_* (\tau^2 + h^{2k-2}),$$

where C_* is a positive constant independent of n, h and τ .

Proof. To establish (4.16), the following estimate

$$(4.17) \quad \|e_u^n\|_{L^\infty} \leq M, \quad \forall 0 \leq n \leq N,$$

will be invoked iteratively. Both (4.16) and (4.17) are proven for $n = 0, \dots, N$ by mathematical induction. At the initial time step,

$$e_{\boldsymbol{\sigma}}^0 = \Pi_h \boldsymbol{\sigma}^0 - \boldsymbol{\sigma}_h^0 = 0, \quad e_u^0 = \Pi_h u^0 - u_h^0 = 0.$$

This shows that (4.16) and (4.17) hold for $n = 0$. Assuming that (4.16) and (4.17) hold for $n - 1$, it remains to verify that both (4.16) and (4.17) hold for n .

Step 1 derives the error equation of $e_{\boldsymbol{\sigma}}^n$ and e_u^n . At time t^n , (3.4) leads to

$$\begin{cases} \left(\frac{\partial u}{\partial t} \Big|_{t^n}, v_h \right) + (\text{divDiv } \boldsymbol{\sigma}^n, v_h) = 0, & \forall v_h \in V_h, \\ (\boldsymbol{\sigma}^n, \boldsymbol{\tau}_h) - (\text{divDiv } \boldsymbol{\tau}_h, u^n) = \left(-\frac{1}{\varepsilon^2} f(u^n) \mathbf{I}, \boldsymbol{\tau}_h \right), & \forall \boldsymbol{\tau}_h \in \Sigma_h. \end{cases}$$

The combination with (4.4) yields

$$(4.18) \quad \begin{cases} (D_\tau u^n, v_h) + (\operatorname{div} \operatorname{Div} \Pi_h \boldsymbol{\sigma}^n, v_h) = (R_1^n, v_h), & \forall v_h \in V_h, \\ (\Pi_h \boldsymbol{\sigma}^n, \boldsymbol{\tau}_h) - (\operatorname{div} \operatorname{Div} \boldsymbol{\tau}_h, \Pi_h u^n) = (R_2^n, \boldsymbol{\tau}_h) + \left(-\frac{1}{\varepsilon^2} f(u^{n-1}) \mathbf{I}, \boldsymbol{\tau}_h\right), & \forall \boldsymbol{\tau}_h \in \Sigma_h \end{cases}$$

with

$$D_\tau u^n := \frac{u^n - u^{n-1}}{\tau}, \quad R_1^n := D_\tau u^n - \frac{\partial u}{\partial t} \Big|_{t^n}, \quad R_2^n := \frac{1}{\varepsilon^2} f(u^{n-1}) \mathbf{I} - \frac{1}{\varepsilon^2} f(u^n) \mathbf{I}.$$

Subtracting the fully discrete scheme (4.3) from (4.18) shows

$$(4.19) \quad \begin{cases} (D_\tau e_u^n, v_h) + (\operatorname{div} \operatorname{Div} e_\sigma^n, v_h) = -(D_\tau \theta_u^n, v_h) + (R_1^n, v_h), & \forall v_h \in V_h, \\ (e_\sigma^n, \boldsymbol{\tau}_h) - (\operatorname{div} \operatorname{Div} \boldsymbol{\tau}_h, e_u^n) = (R_2^n, \boldsymbol{\tau}_h) + (R_3^n, \boldsymbol{\tau}_h), & \forall \boldsymbol{\tau}_h \in \Sigma_h \end{cases}$$

with

$$R_3^n := \frac{1}{\varepsilon^2} f(u_h^{n-1}) \mathbf{I} - \frac{1}{\varepsilon^2} f(u^{n-1}) \mathbf{I}.$$

Taking $(\boldsymbol{\tau}_h, v_h) = (e_\sigma^n, e_u^n)$ in (4.19) and summing up the results lead to the following error equation

$$(4.20) \quad (D_\tau e_u^n, e_u^n) + \|e_\sigma^n\|_{L^2}^2 = -(D_\tau \theta_u^n, e_u^n) + (R_1^n, e_u^n) + (R_2^n, e_\sigma^n) + (R_3^n, e_\sigma^n).$$

Step 2 estimates the terms on the right hand side of (4.20). For the first term of (4.20), the Taylor expansion with $\xi_1 \in (t^{n-1}, t^n)$, (4.12b), and (4.14) lead to

$$(4.21) \quad \begin{aligned} -(D_\tau \theta_u^n, e_u^n) &\leq \|D_\tau \theta_u^n\|_{L^2} \|e_u^n\|_{L^2} = \left\| \frac{\partial \theta_u}{\partial t}(\mathbf{x}, \xi_1) \right\|_{L^2} \|e_u^n\|_{L^2} \\ &\leq C_1 h^{k-1} \left\| \frac{\partial u}{\partial t}(\mathbf{x}, \xi_1) \right\|_{H^{k+1}} \|e_u^n\|_{L^2} \leq C_1 M h^{k-1} \|e_u^n\|_{L^2} \end{aligned}$$

with some constant C_1 from Lemma 4.7. For the second term of (4.20), the Taylor expansion with $\xi_2 \in (t^{n-1}, t^n)$ and (4.14) give rise to

$$(4.22) \quad \begin{aligned} (R_1^n, e_u^n) &= \left(-\frac{1}{2} \frac{\partial^2 u}{\partial t^2}(\mathbf{x}, \xi_2) \tau, e_u^n\right) \leq \frac{1}{2} \left\| \frac{\partial^2 u}{\partial t^2}(\mathbf{x}, \xi_2) \tau \right\|_{L^2} \|e_u^n\|_{L^2} \\ &= \frac{1}{2} \tau \left\| \frac{\partial^2 u}{\partial t^2}(\mathbf{x}, \xi_2) \right\|_{L^2} \|e_u^n\|_{L^2} \leq \frac{1}{2} M \tau \|e_u^n\|_{L^2}. \end{aligned}$$

For the third term of (4.20), the Taylor expansion with $\xi_3 \in (t^{n-1}, t^n)$ and (4.14) show

$$(4.23) \quad \begin{aligned} (R_2^n, e_\sigma^n) &= \frac{1}{\varepsilon^2} (f(u^{n-1}) - f(u^n), \operatorname{tr} e_\sigma^n) = \frac{1}{\varepsilon^2} \left(\frac{\partial(u^3 - u)}{\partial t}(\mathbf{x}, \xi_3) \tau, \operatorname{tr} e_\sigma^n \right) \\ &\leq \frac{1}{\varepsilon^2} \tau \|3u^2 - 1\|_{L^\infty} \left\| \frac{\partial u}{\partial t}(\mathbf{x}, \xi_3) \right\|_{L^2} \|\operatorname{tr} e_\sigma^n\|_{L^2} \leq \frac{3}{\varepsilon^2} M^3 \tau \|\operatorname{tr} e_\sigma^n\|_{L^2}. \end{aligned}$$

Since (4.17) holds for $n-1$, it follows from Lemma 4.8, (4.12c) and (4.14) that

$$\begin{aligned} \|u_h^{n-1}\|_{L^\infty} &\leq \|e_u^{n-1}\|_{L^\infty} + \|\theta_u^{n-1}\|_{L^\infty} + \|u^{n-1}\|_{L^\infty} \\ &\leq M + C_1 C_2 h^{k-3} M + M = C_3 M \end{aligned}$$

with some constant C_2 from Lemma 4.8 and $C_3 = C_1 C_2 h^{k-3} + 2$. This shows

$$\begin{aligned} (R_3^n, e_\sigma^n) &= \frac{1}{\varepsilon^2} ((u_h^{n-1} - u^{n-1}) ((u_h^{n-1})^2 + (u^{n-1})^2 + u_h^{n-1} u^{n-1} - 1), \text{tr } e_\sigma^n) \\ &\leq \frac{1}{\varepsilon^2} (C_3^2 M^2 + M^2 + C_3 M^2) \|\theta_u^{n-1} + e_u^{n-1}\|_{L^2} \|\text{tr } e_\sigma^n\|_{L^2} \\ &\leq \frac{1}{\varepsilon^2} C_4 M^2 \|e_u^{n-1}\|_{L^2} \|\text{tr } e_\sigma^n\|_{L^2} + \frac{1}{\varepsilon^2} C_4 M^2 \|\theta_u^{n-1}\|_{L^2} \|\text{tr } e_\sigma^n\|_{L^2} \end{aligned}$$

with $C_4 = C_3 + C_3^2 + 1$. This and (4.12a) lead to the upper bound of the last term of (4.20) by

$$(4.24) \quad (R_3^n, e_\sigma^n) \leq \frac{1}{\varepsilon^2} C_4 M^2 \|e_u^{n-1}\|_{L^2} \|\text{tr } e_\sigma^n\|_{L^2} + \frac{1}{\varepsilon^2} C_1 C_4 M^3 h^{k-1} \|\text{tr } e_\sigma^n\|_{L^2}.$$

Step 3 proves the estimate (4.16). The substitution of (4.21)-(4.24) into (4.20) shows

$$(4.25) \quad \begin{aligned} (D_\tau e_u^n, e_u^n) + \|e_\sigma^n\|_{L^2}^2 &\leq C_1 M h^{k-1} \|e_u^n\|_{L^2} + \frac{1}{2} M \tau \|e_u^n\|_{L^2} + \frac{3}{\varepsilon^2} M^3 \tau \|\text{tr } e_\sigma^n\|_{L^2} \\ &\quad + \frac{1}{\varepsilon^2} C_4 M^2 \|e_u^{n-1}\|_{L^2} \|\text{tr } e_\sigma^n\|_{L^2} + \frac{1}{\varepsilon^2} C_1 C_4 M^3 h^{k-1} \|\text{tr } e_\sigma^n\|_{L^2}. \end{aligned}$$

Note that $\|\text{tr } e_\sigma^n\|_{L^2}^2 \leq d \|e_\sigma^n\|_{L^2}^2$ with $d = 2, 3$. For any $\delta > 0$, this, (4.25) and Young's inequality imply

$$(4.26) \quad \begin{aligned} (D_\tau e_u^n, e_u^n) + \|e_\sigma^n\|_{L^2}^2 &\leq \left(\frac{C_1^2 M^2}{2} + \frac{M^2}{8} + \frac{9M^6}{4\varepsilon^4 \delta} + \frac{C_1^2 C_4^2 M^6}{4\varepsilon^4 \delta} \right) (\tau^2 + h^{2k-2}) \\ &\quad + \|e_u^n\|_{L^2}^2 + \frac{C_4^2 M^4}{4\varepsilon^4 \delta} \|e_u^{n-1}\|_{L^2}^2 + 3d\delta \|e_\sigma^n\|_{L^2}^2. \end{aligned}$$

Let

$$C_5 = \max \left\{ \frac{C_1^2 M^2}{2} + \frac{M^2}{8} + \frac{9M^6}{4\varepsilon^4 \delta} + \frac{C_1^2 C_4^2 M^6}{4\varepsilon^4 \delta}, 1, \frac{C_4^2 M^4}{4\varepsilon^4 \delta} \right\}.$$

This and (4.26) yield

$$(4.27) \quad (D_\tau e_u^n, e_u^n) + (1 - 3d\delta) \|e_\sigma^n\|_{L^2}^2 \leq C_5 (\tau^2 + h^{2k-2}) + C_5 \|e_u^n\|_{L^2}^2 + C_5 \|e_u^{n-1}\|_{L^2}^2.$$

Taking $\delta < \frac{1}{3d}$ and multiplying $\frac{1}{1-3d\delta} > 1$ on both side of (4.27), the summation from 1 to n leads to

$$\|e_u^n\|_{L^2}^2 + \tau \sum_{i=1}^n \|e_\sigma^i\|_{L^2}^2 \leq \tau C_6 \sum_{i=1}^n \|e_u^i\|_{L^2}^2 + \tau C_6 \sum_{i=1}^n (\tau^2 + h^{2k-2})$$

with $C_6 = \frac{2C_5}{1-3d\delta}$. If τ is sufficiently small such that $C_6 \tau \leq \frac{1}{2}$, then Lemma 2.2 shows

$$\begin{aligned} \|e_u^n\|_{L^2}^2 + \tau \sum_{i=1}^n \|e_\sigma^i\|_{L^2}^2 &\leq \exp\left(\frac{TC_6}{1-C_6\tau}\right) \left(\tau C_6 \sum_{i=1}^n (\tau^2 + h^{2k-2}) \right) \\ &\leq C_6 T \exp(2TC_6) (\tau^2 + h^{2k-2}). \end{aligned}$$

The choice of $C_* \geq C_6 T \exp(2TC_6)$ concludes that (4.16) holds for n .

Step 4 proves $\|e_u^n\|_{L^\infty} \leq M$. If $\tau \leq h^{k-1}$, then an inverse estimate and (4.16) show

$$(4.28) \quad \|e_u^n\|_{L^\infty} \leq h^{-\frac{d}{2}} \|e_u^n\|_{L^2} \leq h^{-\frac{d}{2}} \sqrt{C_*(\tau^2 + h^{2k-2})} \leq \sqrt{2C_*} h^{k-1-\frac{d}{2}}.$$

If $\tau \geq h^{k-1}$, then Lemma 4.8, Lemma 4.1, (4.18) and (4.3) lead to

$$(4.29) \quad \begin{aligned} \|e_u^n\|_{L^\infty} &\leq C_2 |e_u^n|_{2,h} \leq \frac{C_2}{\beta} \sup_{\boldsymbol{\tau}_h^n \in \Sigma_h} \frac{(e_u^n, \operatorname{div} \operatorname{Div} \boldsymbol{\tau}_h^n)}{\|\boldsymbol{\tau}_h^n\|_{L^2}} \\ &= \frac{C_2}{\beta} \sup_{\boldsymbol{\tau}_h^n \in \Sigma_h} \left(\frac{(e_\sigma^n, \boldsymbol{\tau}_h^n)}{\|\boldsymbol{\tau}_h^n\|_{L^2}} + \frac{(f(u^n) - f(u_h^{n-1}), \operatorname{tr} \boldsymbol{\tau}_h^n)}{\varepsilon^2 \|\boldsymbol{\tau}_h^n\|_{L^2}} \right) \\ &\leq \frac{C_2}{\beta} \|e_\sigma^n\|_{L^2} + \frac{C_2 \sqrt{d}}{\varepsilon^2 \beta} \|f(u^n) - f(u_h^{n-1})\|_{L^2}. \end{aligned}$$

For the first term on the right hand side of (4.29), (4.16) shows

$$(4.30) \quad \|e_\sigma^n\|_{L^2} \leq \tau^{-\frac{1}{2}} \sqrt{\tau \|e_\sigma^n\|_{L^2}^2} \leq \tau^{-\frac{1}{2}} \sqrt{C_*(\tau^2 + h^{2k-2})} \leq \sqrt{2C_*} \tau^{\frac{1}{2}}.$$

A triangle inequality, (4.23)-(4.24) plus (4.16) imply

$$(4.31) \quad \begin{aligned} \|f(u^n) - f(u_h^{n-1})\|_{L^2} &\leq \|f(u^n) - f(u^{n-1})\|_{L^2} + \|f(u^{n-1}) - f(u_h^{n-1})\|_{L^2} \\ &\leq 3M^3 \tau + C_4 M^2 \|e_u^{n-1}\|_{L^2} + C_1 C_4 M^3 h^{k-1} \\ &\leq 3M^3 \tau + C_4 M^2 \tau \sqrt{2C_*} + C_1 C_4 M^3 h^{k-1}. \end{aligned}$$

The substitution of (4.30)-(4.31) into (4.29) gives

$$(4.32) \quad \|e_u^n\|_{L^\infty} \leq \frac{C_2}{\beta} \sqrt{2C_*} \tau^{\frac{1}{2}} + \frac{C_2 \sqrt{d}}{\varepsilon^2 \beta} \left((3 + C_1 C_4) M^3 + C_4 M^2 \sqrt{2C_*} \right) \tau.$$

Consequently, (4.28) and (4.32) show that there exist sufficiently small constants τ_0 and h_0 such that $\|e_u^n\|_{L^\infty} \leq M$ holds for any $\tau \leq \tau_0$ and $h \leq h_0$. This concludes the proof. \square

The theorem below follows immediately from Lemma 4.7 and Theorem 4.9.

THEOREM 4.10. *Under the conditions in Theorem 4.9, (4.3) is uniquely solvable with $k \geq 3$ and the following error estimate holds*

$$(4.33) \quad \max_{0 \leq n \leq N} \left(\|u_h^n - u^n\|_{L^2}^2 + \tau \sum_{i=1}^n \|\boldsymbol{\sigma}_h^i - \boldsymbol{\sigma}^i\|_{L^2}^2 \right) \leq C (\tau^2 + h^{2k-2}),$$

where C is a positive constant independent of n, h and τ .

5. Numerical Results. This section presents several numerical examples in two and three dimensions to test the performance of the mixed finite element method. The discrete finite element spaces Σ_h and V_h with $k = 3$ in Section 4 are used.

5.1. Accuracy test in 2D. Let $\Omega = (0, 1)^2$ be a square domain. Consider an analytical solution of (1.1) as

$$u(\mathbf{x}, t) = u(x, y, t) = \exp(-t) \cos(\pi x) \cos(\pi y).$$

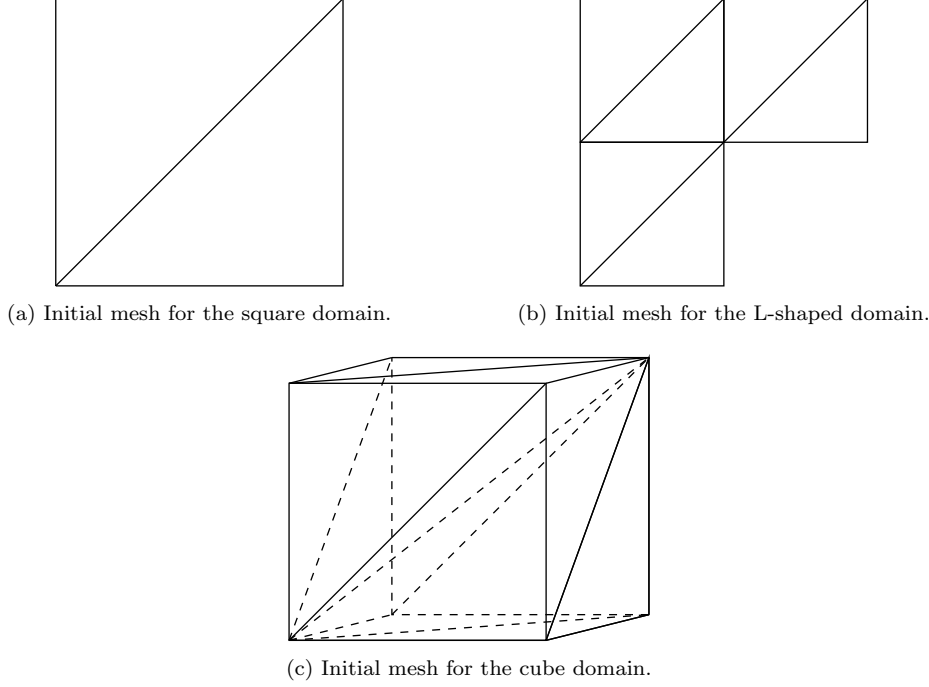


Fig. 1: Initial meshes.

The source term g and boundary terms g_1, g_2 in (1.1) are chosen correspondingly. The initial triangulation is shown in Figure 1a. Each triangulation is refined into a half-sized triangulation uniformly, to get a higher level triangulation. In this example, take $\varepsilon = 1$, and choose $\tau = 1\text{E} - 5$ small enough and $\tau = h^2$, respectively. Table 1 records the errors $\|\boldsymbol{\sigma}^N - \boldsymbol{\sigma}_h^N\|_{L^2}$, $\|u^N - u_h^N\|_{L^2}$, and the convergence rates for the discrete scheme (4.3) with $k = 3$. From Table 1, one can observe that both the convergence rates for $\boldsymbol{\sigma}_h$ and u_h equal 2. This coincides with Theorem 4.10.

5.2. Postprocessing. This subsection provides a postprocessing technique to improve the convergence rates of $\boldsymbol{\sigma}_h$ and u_h . Define the piecewise polynomial space

$$\hat{V}_h := \{q_h \in L^2(\Omega) : q_h|_K \in P_{k+2}(K), \forall K \in \mathcal{T}_h\}.$$

For the time step $n \leq N - 1$, $(\boldsymbol{\sigma}_h^n, u_h^n)$ is obtained from (4.3). Define $\tilde{u}_h^{N-1} \in \hat{V}_h$ satisfying

$$(5.1) \quad \begin{cases} (\tilde{u}_h^{N-1}, v_h)_K = (u_h^{N-1}, v_h)_K, & \forall v_h \in V_h, \\ (\nabla^2 \tilde{u}_h^{N-1}, \nabla^2 q_h)_K = (\boldsymbol{\sigma}_h^{N-1}, \nabla^2 q_h)_K + \left(\frac{1}{\varepsilon^2} f(u_h^{N-1}) \mathbf{I}, \nabla^2 q_h\right)_K, & \forall q_h \in \hat{V}_h, \end{cases}$$

for each $K \in \mathcal{T}_h$. With \tilde{u}_h^{N-1} from (5.1), the improved scheme of (4.3) reads: Find $(\boldsymbol{\sigma}_h^N, u_h^N)$ such that

$$(5.2) \quad \begin{cases} \frac{1}{\tau}(u_h^N, v_h) + (\operatorname{div}\operatorname{Div} \boldsymbol{\sigma}_h^N, v_h) = \frac{1}{\tau}(\tilde{u}_h^{N-1}, v_h), & \forall v_h \in V_h, \\ (\boldsymbol{\sigma}_h^N, \boldsymbol{\tau}_h) - (\operatorname{div}\operatorname{Div} \boldsymbol{\tau}_h, u_h^N) = (-\frac{1}{\varepsilon^2}f(\tilde{u}_h^{N-1})\mathbf{I}, \boldsymbol{\tau}_h), & \forall \boldsymbol{\tau}_h \in \Sigma_h. \end{cases}$$

Then, the post-processed solution \tilde{u}_h^N can be derived using an analogy scheme (5.1) at time t^N . Table 2 shows that the convergence rates for $\boldsymbol{\sigma}_h$ and \tilde{u}_h can be improved to 4, while the convergence rate for u_h equals 2.

Table 1: Errors on the square domain.

Mesh	$\ \boldsymbol{\sigma}^N - \boldsymbol{\sigma}_h^N\ _{L^2}$	Rate	$\ u^N - u_h^N\ _{L^2}$	Rate
$\varepsilon = 1, \tau = 1\text{E} - 5, T = 2\text{E} - 4$				
1	3.26E+00	-	2.69E-01	-
2	2.61E-01	3.64	7.37E-02	1.87
3	2.62E-02	3.32	1.95E-02	1.92
4	4.46E-03	2.56	4.95E-03	1.98
5	1.07E-03	2.05	1.24E-03	1.99
6	2.68E-04	2.00	3.11E-04	2.00
$\varepsilon = 1, \tau = h^2, T = 1$				
1	1.18E+00	-	1.06E-01	-
2	1.02E-01	3.54	2.71E-02	1.97
3	1.23E-02	3.04	7.17E-03	1.92
4	2.69E-03	2.19	1.82E-03	1.98
5	6.71E-04	2.00	4.58E-04	1.99

Table 2: Errors on the square domain with postprocessing.

Mesh	$\ \boldsymbol{\sigma}^N - \boldsymbol{\sigma}_h^N\ _{L^2}$	Rate	$\ u^N - u_h^N\ _{L^2}$	Rate	$\ u^N - \tilde{u}_h^N\ _{L^2}$	Rate
$\varepsilon = 1, \tau = 1\text{E} - 6, T = 4\text{E} - 5$						
1	3.27E+00	-	2.69E-01	-	1.32E-01	-
2	2.64E-01	3.63	7.37E-02	1.87	9.86E-03	3.74
3	2.05E-02	3.69	1.95E-02	1.92	7.47E-04	3.72
4	1.37E-03	3.90	4.95E-03	1.98	4.83E-05	3.95
$\varepsilon = 1, \tau = h^4, T = 1$						
1	1.95E+00	-	1.79E-01	-	1.09E-01	-
2	1.57E-01	3.63	4.48E-02	1.99	6.63E-03	4.04
3	1.16E-02	3.75	1.18E-02	1.92	4.34E-04	3.93
4	7.68E-04	3.92	3.00E-03	1.98	2.89E-05	3.91

5.3. Accuracy test on the L-shaped domain. Let $\Omega = (-1, 1)^2 \setminus ([0, 1] \times [-1, 0])$ be an L-shaped domain. Consider an analytical solution of (1.1) as

$$u(\mathbf{x}, t) = u(r, \theta, t) = \exp(-t)r^{\frac{4}{3}}\cos(\frac{2}{3}\theta).$$

The function g and boundary conditions g_1 and g_2 are chosen correspondingly. The initial triangulation is shown in Figure 1b. In this example, take $\varepsilon = 1$, and choose $\tau = 1\text{E}-5$ small enough and $\tau = h^2$, respectively. Table 3 records the errors $\|\boldsymbol{\sigma}^N - \boldsymbol{\sigma}_h^N\|_{L^2}$, $\|u^N - u_h^N\|_{L^2}$, and the convergence rates for the discrete scheme (4.3) with $k = 3$. From Table 3, the convergence can still be observed on the L-shaped domain. The convergence rates are degenerate because the solution possesses singularity at the origin. The rate equals 0.33 for $\boldsymbol{\sigma}_h$ and 0.66 for u_h .

Table 3: Errors on the L-shaped domain.

Mesh	$\ \boldsymbol{\sigma}^N - \boldsymbol{\sigma}_h^N\ _{L^2}$	Rate	$\ u^N - u_h^N\ _{L^2}$	Rate
$\varepsilon = 1, \tau = 1\text{E} - 5, T = 2\text{E} - 4$				
1	2.81E+00	-	5.53E-01	-
2	1.96E+00	0.52	3.78E-01	0.55
3	1.44E+00	0.45	2.52E-01	0.59
4	1.09E+00	0.40	1.62E-01	0.64
5	8.44E-01	0.37	1.00E-01	0.69
$\varepsilon = 1, \tau = h^2, T = 1$				
1	7.05E-01	-	2.64E-01	-
2	5.89E-01	0.26	1.85E-01	0.51
3	4.71E-01	0.32	1.20E-01	0.63
4	3.75E-01	0.33	7.50E-02	0.68
5	2.98E-01	0.33	4.56E-02	0.72

5.4. Accuracy test in 3D. Let $\Omega = (0, 1)^3$ be a cubic domain. Consider an analytical solution of (1.1) as

$$u(\mathbf{x}, t) = u(x, y, z, t) = \exp(-t) \cos(\pi x) \cos(\pi y) \cos(\pi z).$$

The source term g and boundary terms g_1, g_2 in (1.1) are chosen correspondingly. The initial triangulation is shown in Figure 1c. In this example, take $\varepsilon = 1$, and choose $\tau = 1\text{E} - 5$ small enough and $\tau = h^2$, respectively. Table 4 records the errors $\|\boldsymbol{\sigma}^N - \boldsymbol{\sigma}_h^N\|_{L^2}$, $\|u^N - u_h^N\|_{L^2}$, and the convergence rates for the discrete scheme (4.3) with $k = 3$. Table 4 shows that the convergence rate for u_h equals 2. This coincides with Theorem 4.10.

5.5. Coalescence of two drops. Consider the coalescence of two material drops governed by the Cahn-Hilliard equation (1.1). Assume that, at time $t = 0$, the first material occupies two circular regions that are right next to each other and the second material fills the rest of the domain. The two regions of the first material then coalesce with each other to form a single drop under the Cahn-Hilliard dynamics. The initial distribution for the materials from [55] reads

$$u_0(\mathbf{x}) = 1 - \tanh \frac{|\mathbf{x} - \mathbf{x}_0| - R_0}{\sqrt{2}\varepsilon} - \tanh \frac{|\mathbf{x} - \mathbf{x}_1| - R_0}{\sqrt{2}\varepsilon},$$

where $\varepsilon = 0.01$ is the characteristic inter-facial thickness, $\mathbf{x}_0 = (0.3, 0.5)$ and $\mathbf{x}_1 = (0.7, 0.5)$ are the centers of the circular regions for the first material, and $R_0 = 0.19$ is the radius of these circles. Set $g = 0, g_1 = 0, g_2 = 0$ of (1.1) for simulation of

Table 4: Errors on the cube domain.

Mesh	$\ \sigma^N - \sigma_h^N\ _{L^2}$	Rate	$\ u^N - u_h^N\ _{L^2}$	Rate
$\varepsilon = 1, \tau = 1E-5, T = 2E-4$				
1	4.89E+00	-	2.45E-01	-
2	4.87E-01	3.33	6.41E-02	1.94
3	4.07E-02	3.58	1.73E-02	1.89
4	4.91E-03	3.05	4.42E-03	1.97
$\varepsilon = 1, \tau = h^2, T = 1$				
1	1.78E+00	-	9.13E-02	-
2	1.78E-01	3.33	2.36E-02	1.95
3	1.50E-02	3.57	6.35E-03	1.89

natural phenomena. The process of coalescence of the two drops is demonstrated in Figure 2 with a temporal sequence of snapshots of the interfaces between the materials (visualized by the contour level $u = 0$).

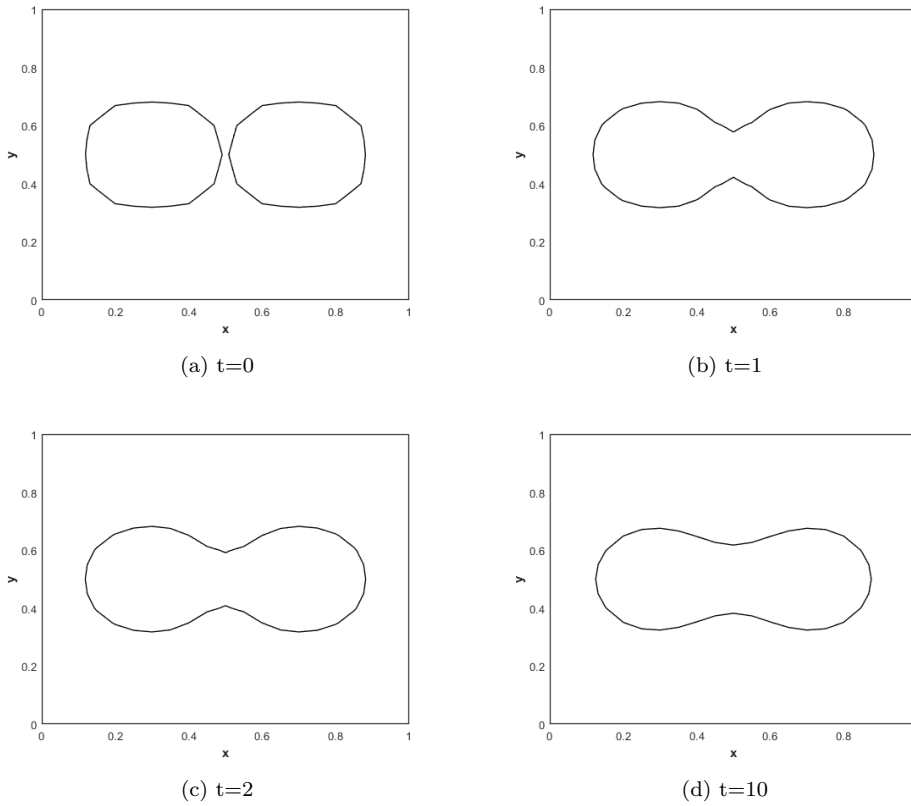


Fig. 2: Temporal sequence of snapshots for the coalescence of two drops. Results are obtained with $\tau = 1E-2$ and $h = \sqrt{2}/20$.

5.6. Biharmonic equation on the L-shaped domain. This example compares the new mixed method [40], the Morley method [45] and the Ciarlet-Raviart method [18] for biharmonic equations with Cahn-Hilliard boundary conditions on the L-shaped domain. Consider the biharmonic equation

$$(5.3) \quad \begin{cases} \Delta^2 u = g, & \text{in } \Omega, \\ \partial_n u = g_1, & \text{on } \partial\Omega, \\ \partial_n(\Delta u) = g_2, & \text{on } \partial\Omega. \end{cases}$$

The L-shaped domain Ω , the analytical solution at $t = 0$ and the initial triangulation from Subsection 5.3 are used. The function g and boundary conditions g_1 and g_2 in (5.3) are chosen correspondingly.

In this subsection, with an abuse of notation, define $\boldsymbol{\sigma} := \nabla^2 u$ for the new mixed method and the Morley method, and define $\boldsymbol{\sigma} := \Delta u$ for the Ciarlet-Raviart method. Table 5 records the errors $\|\boldsymbol{\sigma} - \boldsymbol{\sigma}_h\|_{L^2}$ and $\|u - u_h\|_{L^2}$ by these three methods. The Ciarlet-Raviart method using piecewise continuous linear functions does not converge, while the new mixed method and the Morley method do converge on the L-shaped domain. The convergence rates are degenerate because the solution possesses singularity at the origin.

Table 5: Errors on the L-shaped domain for the biharmonic equation with Cahn-Hilliard boundary conditions.

Mesh	$\ \boldsymbol{\sigma} - \boldsymbol{\sigma}_h\ _{L^2}$	Rate	$\ u - u_h\ _{L^2}$	Rate
New mixed method (P3-P1)				
1	1.75E+00	-	5.78E-01	-
2	1.45E+00	0.28	3.86E-01	0.59
3	1.19E+00	0.28	2.57E-01	0.59
4	9.75E-01	0.29	1.66E-01	0.63
5	7.90E-01	0.30	1.04E-01	0.67
6	6.38E-01	0.31	6.34E-02	0.72
Morley method (P2)				
1	1.86E+00	-	5.76E-01	-
2	1.61E+00	0.21	4.56E-01	0.34
3	1.36E+00	0.25	3.25E-01	0.48
4	1.12E+00	0.28	2.22E-01	0.55
5	9.11E-01	0.30	1.47E-01	0.60
6	7.33E-01	0.31	9.53E-02	0.62
Ciarlet-Raviart method (P1-P1)				
1	3.10E+00	-	1.40E+00	-
2	3.36E+00	-	1.88E+00	-
3	3.49E+00	-	2.07E+00	-
4	3.55E+00	-	2.15E+00	-
5	3.58E+00	-	2.18E+00	-
6	3.60E+00	-	2.19E+00	-

Next, consider the eigenvalue problem corresponding to (5.3). Table 6 records the first six smallest nonzero eigenvalues obtained by these three methods. The first

eigenvalue by the Ciarlet-Raviart method is different from those by the new finite element method and the Morley method.

Table 6: Eigenvalues of the biharmonic operator on the L-shaped domain.

Mesh	1st	2nd	3rd	4th	5th
The new mixed FEM (P3-P1)					
1	7.1399	11.7918	97.4396	97.4396	128.7678
2	8.0275	12.0402	97.4113	97.4113	129.0807
3	8.7681	12.2025	97.4103	97.4103	129.3118
4	9.3379	12.3072	97.4132	97.4132	129.4666
5	9.7498	12.3742	97.4252	97.4252	129.5834
Morley FEM (P2)					
1	6.6167	10.8045	81.4404	84.6007	107.3816
2	7.5927	11.6734	92.7873	93.7330	122.6000
3	8.4162	12.0429	96.2045	96.4536	127.5163
4	9.0711	12.2249	97.1047	97.1678	128.9456
5	9.5588	12.3266	97.3328	97.3486	129.3880
Ciarlet-Raviart FEM (P1-P1)					
1	2.3897	13.0454	107.4661	107.5314	146.6509
2	2.2528	12.6333	99.9091	99.9153	133.9467
3	2.2055	12.5260	98.0344	98.0349	130.7807
4	2.1881	12.4986	97.5655	97.5655	129.9860
5	2.1816	12.4917	97.4482	97.4482	129.7868

6. Concluding remarks. This paper developed a new mixed finite method for the Cahn-Hilliard equation. The well-posedness of the mixed formulation was provided by proving its equivalence with the primal formulation. The error estimates of the linearized fully discrete scheme was established by mathematical induction. The boundedness of $\|u_h\|_{L^\infty}$ was proved. Additionally, some postprocessing technique was given to improve the convergence rates which was verified by numerical tests. The comparison with the Ciarlet-Raviart method for biharmonic equations with Cahn-Hilliard boundary conditions was provided.

Since the Cahn-Hilliard equation describes the dissipation of the Cahn-Hilliard free energy [57] in a conservative system, it is desirable for a numerical scheme to preserve this energy property. One future work will investigate the discrete energy of the current mixed finite element method. Besides, this paper has only discussed the case with the interface parameter $\varepsilon = 1$. However, a small $\varepsilon \ll 1$ is important in applications and brings difficulties in computation. The numerical schemes when ε approaches zero will be discussed in the future work.

REFERENCES

- [1] H. ABELS, *On a diffuse interface model for two-phase flows of viscous, incompressible fluids with matched densities*, Arch. Ration. Mech. Anal., 194 (2009), pp. 463–506.
- [2] R. A. ADAMS AND J. J. FOURNIER, *Sobolev spaces*, Elsevier, 2003.
- [3] C. AMROUCHE, P. G. CIARLET, L. GRATIE, AND S. KESAVAN, *On the characterizations of matrix fields as linearized strain tensor fields*, J. Math. Pures Appl., 86 (2006), pp. 116–132.

- [4] D. M. ANDERSON, G. B. MCFADDEN, AND A. A. WHEELER, *Diffuse-interface methods in fluid mechanics*, in Annual review of fluid mechanics, Vol. 30, vol. 30 of Annu. Rev. Fluid Mech., Annual Reviews, Palo Alto, CA, 1998, pp. 139–165.
- [5] P. F. ANTONIETTI, L. B. DA VEIGA, S. SCACCHI, AND M. VERANI, *A C^1 virtual element method for the Cahn-Hilliard equation with polygonal meshes*, SIAM J. Numer. Anal., 54 (2016), pp. 34–56.
- [6] A. R. APPADU, J. K. DJOKO, H. H. GIDEY, AND J. M. S. LUBUMA, *Analysis of multilevel finite volume approximation of 2D convective Cahn-Hilliard equation*, Jpn. J. Ind. Appl. Math., 34 (2017), pp. 253–304.
- [7] D. BOFFI, F. BREZZI, M. FORTIN, ET AL., *Mixed finite element methods and applications*, vol. 44, Springer, 2013.
- [8] S. C. BRENNER, M. NEILAN, A. REISER, AND L.-Y. SUNG, *A c^0 interior penalty method for a von kármán plate*, Numer. Math., 135 (2017), pp. 803–832.
- [9] J. W. CAHN, *Phase separation by spinodal decomposition in isotropic systems*, J. Chem. Phys., 42 (1965), pp. 93–99.
- [10] J. W. CAHN AND J. E. HILLIARD, *Free energy of a nonuniform system. I. Interfacial free energy*, J. Chem. Phys., 28 (1958), pp. 258–267.
- [11] C. CARSTENSEN AND S. PUTTKAMMER, *Direct guaranteed lower eigenvalue bounds with optimal a priori convergence rates for the bi-Laplacian*, SIAM J. Numer. Anal., 61 (2023), pp. 812–836.
- [12] F. CHEN AND J. SHEN, *Efficient energy stable schemes with spectral discretization in space for anisotropic Cahn-Hilliard systems*, Commun. Comput. Phys., 13 (2013), pp. 1189–1208.
- [13] L. CHEN AND X. HUANG, *Finite elements for div-and divdiv-conforming symmetric tensors in arbitrary dimension*, SIAM J. Numer. Anal., 60 (2022), pp. 1932–1961.
- [14] L. CHEN AND X. HUANG, *Finite elements for div div conforming symmetric tensors in three dimensions*, Math. Comp., 91 (2022), pp. 1107–1142.
- [15] L. CHEN AND C. XU, *A time splitting space spectral element method for the Cahn-Hilliard equation*, East Asian J. Appl. Math., 3 (2013), pp. 333–351.
- [16] Y. CHEN, Y. HUANG, N. YI, AND P. YIN, *Recovery type a posteriori error estimation of an adaptive finite element method for cahn-hilliard equation*, J. Sci. Comput., 98 (2024), p. 35.
- [17] P. G. CIARLET, *Mathematical elasticity: Three-dimensional elasticity*, SIAM, 2021.
- [18] P. G. CIARLET AND P.-A. RAVIART, *A mixed finite element method for the biharmonic equation*, in Mathematical aspects of finite elements in partial differential equations, Elsevier, 1974, pp. 125–145.
- [19] M. I. M. COPETTI AND C. M. ELLIOTT, *Numerical analysis of the Cahn-Hilliard equation with a logarithmic free energy*, Numer. Math., 63 (1992), pp. 39–65.
- [20] A. E. DIEGEL, C. WANG, AND S. M. WISE, *Stability and convergence of a second-order mixed finite element method for the Cahn-Hilliard equation*, IMA J. Numer. Anal., 36 (2016), pp. 1867–1897.
- [21] Q. DU AND R. A. NICOLAIDES, *Numerical analysis of a continuum model of phase transition*, SIAM J. Numer. Anal., 28 (1991), pp. 1310–1322.
- [22] C. M. ELLIOTT AND D. A. FRENCH, *Numerical studies of the Cahn-Hilliard equation for phase separation*, IMA J. Appl. Math., 38 (1987), pp. 97–128.
- [23] C. M. ELLIOTT AND D. A. FRENCH, *A nonconforming finite-element method for the two-dimensional Cahn-Hilliard equation*, SIAM J. Numer. Anal., 26 (1989), pp. 884–903.
- [24] C. M. ELLIOTT, D. A. FRENCH, AND F. MILNER, *A second order splitting method for the Cahn-Hilliard equation*, Numer. Math., 54 (1989), pp. 575–590.
- [25] C. M. ELLIOTT AND S. LARSSON, *Error estimates with smooth and nonsmooth data for a finite element method for the Cahn-Hilliard equation*, Math. Comp., 58 (1992), pp. 603–630.
- [26] C. M. ELLIOTT AND Z. SONGMU, *On the Cahn-Hilliard equation*, Arch. Ration. Mech. Anal., 96 (1986), pp. 339–357.
- [27] X. FENG, *Fully discrete finite element approximations of the Navier-Stokes-Cahn-Hilliard diffuse interface model for two-phase fluid flows*, SIAM J. Numer. Anal., 44 (2006), pp. 1049–1072.
- [28] X. FENG AND O. KARAKASHIAN, *Fully discrete dynamic mesh discontinuous Galerkin methods for the Cahn-Hilliard equation of phase transition*, Math. Comp., 76 (2007), pp. 1093–1117.
- [29] X. FENG AND S. WISE, *Analysis of a Darcy-Cahn-Hilliard diffuse interface model for the Hele-Shaw flow and its fully discrete finite element approximation*, SIAM J. Numer. Anal., 50 (2012), pp. 1320–1343.
- [30] X. FENG AND H. WU, *A posteriori error estimates for finite element approximations of the cahn-hilliard equation and the hele-shaw flow*, J. Comput. Math., (2008), pp. 767–796.
- [31] T. FÜHRER AND N. HEUER, *Mixed finite elements for kirchhoff-love plate bending*, Math. Comp.,

- (2024). online.
- [32] T. FÜHRER, N. HEUER, AND A. H. NIEMI, *An ultraweak formulation of the Kirchhoff-Love plate bending model and DPG approximation*, *Math. Comp.*, 88 (2019), pp. 1587–1619.
 - [33] D. FURIHATA AND T. MATSUO, *A stable, convergent, conservative and linear finite difference scheme for the Cahn-Hilliard equation*, *Japan J. Indust. Appl. Math.*, 20 (2003), pp. 65–85.
 - [34] E. H. GEORGIOULIS, P. HOUSTON, AND J. VIRTANEN, *An a posteriori error indicator for discontinuous Galerkin approximations of fourth-order elliptic problems*, *IMA J. Numer. Anal.*, 31 (2011), pp. 281–298.
 - [35] V. GIRAULT AND P.-A. RAVIART, *Finite element methods for Navier-Stokes equations: theory and algorithms*, vol. 5, Springer Science & Business Media, 2012.
 - [36] G. GRÜN AND F. KLINGBEIL, *Two-phase flow with mass density contrast: stable schemes for a thermodynamic consistent and frame-indifferent diffuse-interface model*, *J. Comput. Phys.*, 257 (2014), pp. 708–725.
 - [37] J. GUO, C. WANG, S. M. WISE, AND X. YUE, *An H^2 convergence of a second-order convex-splitting, finite difference scheme for the three-dimensional Cahn-Hilliard equation*, *Commun. Math. Sci.*, 14 (2016), pp. 489–515.
 - [38] J. G. HEYWOOD AND R. RANNACHER, *Finite-element approximation of the nonstationary Navier-Stokes problem. IV. Error analysis for second-order time discretization*, *SIAM J. Numer. Anal.*, 27 (1990), pp. 353–384.
 - [39] J. HU, *Finite element approximations of symmetric tensors on simplicial grids in \mathbb{R}^n : the higher order case*, *J. Comput. Math.*, 33 (2015), pp. 283–296.
 - [40] J. HU, R. MA, AND M. ZHANG, *A family of mixed finite elements for the biharmonic equations on triangular and tetrahedral grids*, *Sci. China Math.*, 64 (2021), pp. 2793–2816.
 - [41] J. HU AND S. ZHANG, *A family of conforming mixed finite elements for linear elasticity on triangular grids*, arXiv:1406.7457, (2015).
 - [42] J. HU AND S. ZHANG, *A family of symmetric mixed finite elements for linear elasticity on tetrahedral grids*, *Sci. China Math.*, 58 (2015), pp. 297–307.
 - [43] D. KAY, V. STYLES, AND E. SÜLI, *Discontinuous Galerkin finite element approximation of the Cahn-Hilliard equation with convection*, *SIAM J. Numer. Anal.*, 47 (2009), pp. 2660–2685.
 - [44] H.-G. LEE, J. S. LOWENGRUB, AND J. GOODMAN, *Modeling pinchoff and reconnection in a Hele-Shaw cell. I. The models and their calibration*, *Phys. Fluids*, 14 (2002), pp. 492–513.
 - [45] L. S. D. MORLEY, *The triangular equilibrium element in the solution of plate bending problems*, *Aero. Quart.*, 19 (1968), pp. 149–169.
 - [46] F. NABET, *Convergence of a finite-volume scheme for the Cahn-Hilliard equation with dynamic boundary conditions*, *IMA J. Numer. Anal.*, 36 (2016), pp. 1898–1942.
 - [47] A. NOVICK-COHEN, *The Cahn-Hilliard equation: mathematical and modeling perspectives*, *Adv. Math. Sci. Appl.*, 8 (1998), pp. 965–985.
 - [48] D. PAULY AND W. ZULEHNER, *The divdiv-complex and applications to biharmonic equations*, *Appl. Anal.*, 99 (2020), pp. 1579–1630.
 - [49] K. RAFETSEDER AND W. ZULEHNER, *A decomposition result for Kirchhoff plate bending problems and a new discretization approach*, *SIAM J. Numer. Anal.*, 56 (2018), pp. 1961–1986.
 - [50] Z. Z. SUN, *A second-order accurate linearized difference scheme for the two-dimensional Cahn-Hilliard equation*, *Math. Comp.*, 64 (1995), pp. 1463–1471.
 - [51] J. WANG, Q. ZHAI, R. ZHANG, AND S. ZHANG, *A weak Galerkin finite element scheme for the Cahn-Hilliard equation*, *Math. Comp.*, 88 (2019), pp. 211–235.
 - [52] S. WU AND Y. LI, *Analysis of the Morley element for the Cahn-Hilliard equation and the Hele-Shaw flow*, *ESAIM: Math. Model. Numer. Anal.*, 54 (2020), pp. 1025–1052.
 - [53] Y. XIA, Y. XU, AND C.-W. SHU, *Local discontinuous Galerkin methods for the Cahn-Hilliard type equations*, *J. Comput. Phys.*, 227 (2007), pp. 472–491.
 - [54] X. YANG, J. J. FENG, C. LIU, AND J. SHEN, *Numerical simulations of jet pinching-off and drop formation using an energetic variational phase-field method*, *J. Comput. Phys.*, 218 (2006), pp. 417–428.
 - [55] Z. YANG, L. LIN, AND S. DONG, *A family of second-order energy-stable schemes for Cahn-Hilliard type equations*, *J. Comput. Phys.*, 383 (2019), pp. 24–54.
 - [56] P. YUE, J. J. FENG, C. LIU, AND J. SHEN, *A diffuse-interface method for simulating two-phase flows of complex fluids*, *J. Fluid Mech.*, 515 (2004), pp. 293–317.
 - [57] S. ZHANG AND M. WANG, *A nonconforming finite element method for the Cahn-Hilliard equation*, *J. Comput. Phys.*, 229 (2010), pp. 7361–7372.
 - [58] S. ZHANG AND Z. ZHANG, *Invalidity of decoupling a biharmonic equation to two poisson equations on non-convex polygons*, *Int. J. Numer. Anal. Model.*, 5 (2008), pp. 73–76.
 - [59] S. ZHONGCI AND M. WANG, *Finite Element Methods*, Science Press, 2013.